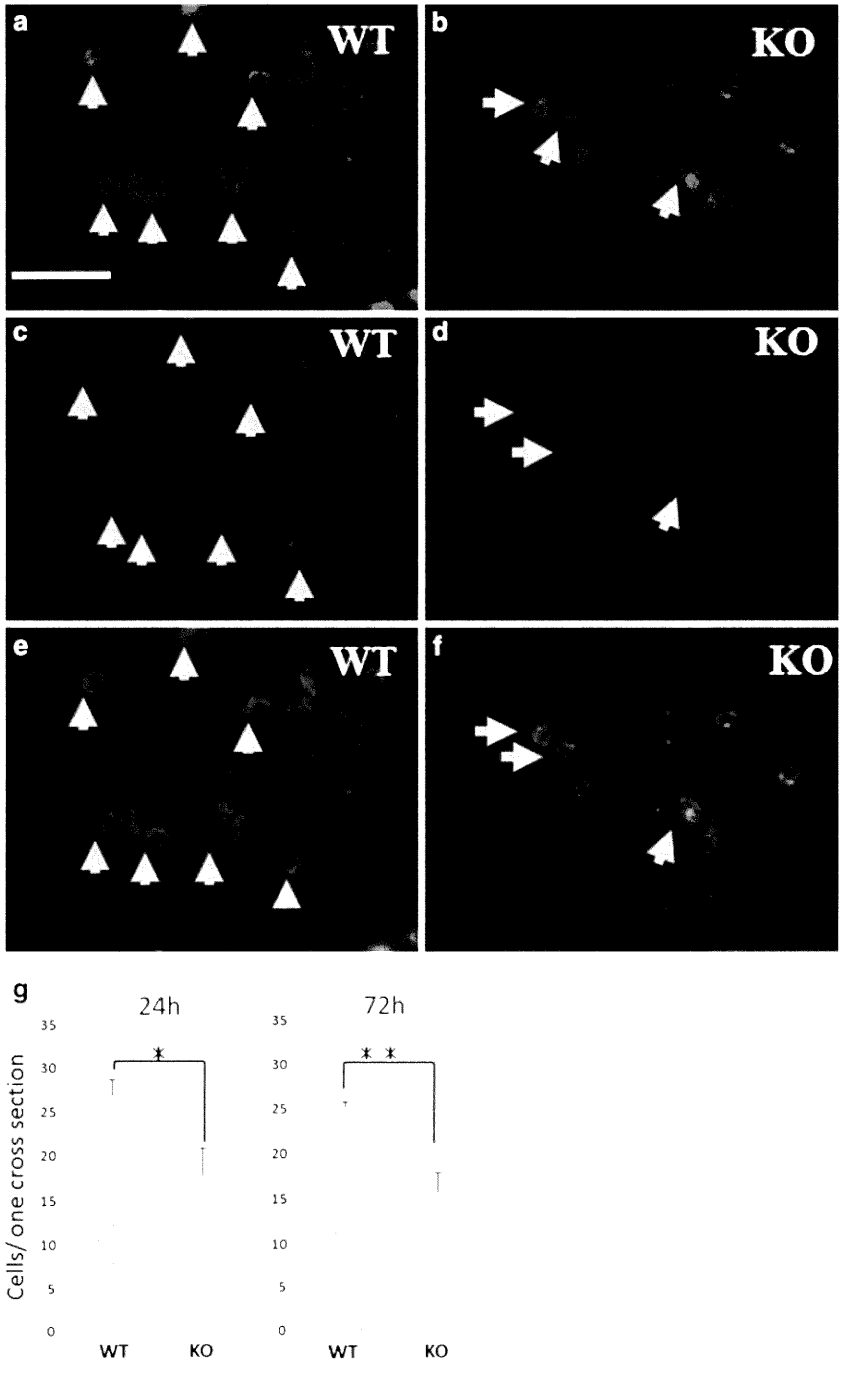

Fig. 4 Fewer NeuN/caspase-3-active double-positive cells were counted in KO mice 24 and 72 h after spinal cord injury (SCI). We counted NeuN/caspase-3-active double-positive cells as apoptotic cells. Double-positive cells were counted and compared between genotypes. **a**–**f** Representative NeuN/caspase-3-active double fluorescent immunostaining 24 h after SCI. NeuN staining (**a**, **b**), caspase-3-active (**c**, **d**), and merged figures in WT and KO mice (**e**, **f**). Fewer neurons were caspase-3-active in KO mice (*arrow*) than WT mice (*arrow heads*). **g** *Bar graphs* show double-positive cell numbers in WT and KO mice 24 h (*left panel*) and 72 h (*right panel*) after spinal cord compression injury. Significantly fewer double-positive cells were counted in KO mice compared with WT mice 24 and 72 h after SCI. $*p < 0.05$, $**p < 0.01$. *Bar* 50 μm for **a**–**f**

Discussion

In this study, deletion of MIF suppressed glutamate-induced neuronal death in vitro. Recombinant human MIF exacerbated glutamate-induced neuronal death in CGN from MIF KO mice. In the in-vivo study, MIF KO mice showed a decreased number of apoptotic neurons, better neuronal survival, and better hind-limb functional recovery compared with WT mice after spinal cord compression injury.

Previously, we examined MIF expression in a mouse spinal cord compression injury model [ ]. Activated microglia with amoeboid morphology that accumulated in the lesion epicenter expressed MIF mRNA and protein, and the peak of MIF expression was three days after injury. In this study, MIF deletion did not change microglia accumulation in the lesion epicenter three days after SCI. In a lipopolysaccharide-mediated endotoxemia model, MIF released from anterior pituitary glands stimulates macrophages and monocytes to secrete inflammatory cytokines

[3]. MIF is a potent inducer of TNF-α [3], IL-1β [17], and IL-6 [16]. Proinflammatory cytokines, which are secreted from macrophages and monocytes, negatively affect neuronal survival after SCI [15]. In this study, the different number of NeuN/caspase-3 positive cells may be a result of cytokine expression differences caused by the absence of MIF from accumulated inflammatory cells.

In the in vitro study, MIF appeared to hinder neuronal survival in WT mice, and recombinant human MIF exacerbated glutamate-induced neuronal death of CGN from KO mice. MIF regulates the proliferation and apoptosis of cells via direct effects on the tumor suppressor protein p53, implicating a role for MIF in synovial hyperplasia [16]. Delayed neuronal cell death after brain trauma is mediated by p53-dependent mechanisms [14]. The number of NeuN/caspase-3-active double-positive cells in KO mice was significantly smaller than in WT mice 24 h and 72 h after injury, suggesting MIF may also facilitate apoptosis of neurons during the first few days after injury by p53-dependent pathways in vivo.

Six-week hind-limb locomotor assessments revealed that KO mice showed significantly better locomotor recovery than WT mice. This result correlates with the histological finding that more neurons survived in KO mice six weeks after SCI. We could also correlate six weeks neuronal counts with neuronal cell death within a few days after injury. Less NeuN/ caspase-3-positive apoptotic cells were counted in KO mice, suggesting that the initial response may determine long-term outcome.

In this study, significant locomotor recovery in KO mice was observed three to six weeks after SCI. The time course recovery of hind-limb function showed statistically significant differences between genotypes in repeated-measures ANOVA ($p < 0.01$). The difference in the recovery curve between genotypes was partially explained by the difference in one to three days neuronal death or six weeks neuron counts. In addition, dorsal skin wound healing was significantly delayed in MIF KO mice compared with WT mice because of a significant reduction in fibroblast and keratinocyte migration, as observed in MIF KO mice after 1-oleoyl-2-lysophosphatidic acid treatment [19]. In the injured spinal cord, a reduction in KO mouse fibroblasts could occur because the excitotoxic properties of glutamate and the ischemic conditions cause acidosis. The difference in hind-limb locomotor score between genotypes may be derived from the wound-healing process of fibroblasts that have migrated to the lesion epicenter after SCI.

The MIF protein is present in astrocyte-like cells in the cerebral white matter and cortex [12]. The signal transductions in KO mouse astrocytes could be somewhat different than in the WT mice because MIF is upregulated in astrocytes seven days after SCI [9]. This difference may cause a glial scar that has a different molecular mechanism of MIF signal transduction in the injured spinal cord. Elucidation of the significantly improved recovery process in KO mice after SCI may facilitate development of new therapeutic approaches in SCI.

Acknowledgments We thank Dr Toshinori Nakayama of Department of Immunology, Graduate School of Medicine, Chiba University, for management of animal supply and useful discussions about this paper.

References

1. Abe R, Shimizu T, Ohkawara A, Nishihira J (2000) Enhancement of macrophage migration inhibitory factor (MIF) expression in injured epidermis and cultured fibroblasts. Biochim Biophys Acta 1500:1–9
2. Akoum A, Kong J, Metz C, Beaumont MC (2002) Spontaneous and stimulated secretion of monocyte chemotactic protein-1 and macrophage migration inhibitory factor by peritoneal macrophages in women with and without endometriosis. Fertil Steril 77:989–994
3. Bernhagen J, Calandra T, Mitchell RA et al (1993) MIF is a pituitary-derived cytokine that potentiates lethal endotoxaemia. Nature 365:756–759
4. Bloom BR, Shevach E (1975) Requirement for T cells in the production of migration inhibitory factor. J Exp Med 142:1306–1311
5. Farooque M (2000) Spinal cord compression injury in the mouse: presentation of a model including assessment of motor dysfunction. Acta Neuropathol 100:13–22
6. Farooque M, Isaksson J, Olsson Y (2001) Improved recovery after spinal cord injury in neuronal nitric oxide synthase-deficient mice but not in TNF-alpha-deficient mice. J Neurotrauma 18:105–114
7. Fujimoto S (1997) Identification of macrophage migration inhibitory factor (MIF) in rat spinal cord and its kinetics on experimental spinal cord injury. Hokkaido Igaku Zasshi 72:409–430 Japanese
8. Honma N, Koseki H, Akasaka T et al (2000) Deficiency of the macrophage migration inhibitory factor gene has no significant effect on endotoxaemia. Immunology 100:84–90
9. Koda M, Nishio Y, Hashimoto M et al (2004) Up-regulation of macrophage migration- inhibitory factor expression after compression-induced spinal cord injury in rats. Acta Neuropathol 108:31–36
10. Niino M, Ogata A, Kikuchi S, Tashiro K, Nishihira J (2000) Macrophage migration inhibitory factor in the cerebrospinal fluid of patients with conventional and optic-spinal forms of multiple sclerosis and neuro-Behçet's disease. J Neurol Sci 179(S 1–2):127–131
11. Nishihira J (1998) Novel pathophysiological aspects of macrophage migration inhibitory factor (review). Int J Mol Med 2:17–28
12. Ogata A, Nishihira J, Suzuki T, Nagashima K, Tashiro K (1998) Identification of macrophage migration inhibitory factor mRNA expression in neural cells of the rat brain by in situ hybridization. Neurosci Lett 246:173–177
13. Oshima S, Onodera S, Amizuka N et al (2006) Macrophage migration inhibitory factor-deficient mice are resistant to ovariectomy-induced bone loss. FEBS Lett 580:1251–1256
14. Plesnila N, von Baumgarten L, Retiounskaia M et al (2007) Delayed neuronal death after brain trauma involves p53-dependent inhibition of NF-kappaB transcriptional activity. Cell Death Differ 14:1529–1541
15. Raivich G, Liu ZQ, Kloss CU et al (2002) Cytotoxic potential of proinflammatory cytokines: combined deletion of TNF receptors TNFR1 and TNFR2 prevents motoneuron cell death after facial axotomy in adult mouse. Exp Neurol 178:186–193

16. Santos LL, Morand EF (2006) The role of macrophage migration inhibitory factor in the inflammatory immune response and rheumatoid arthritis. Wien Med Wochenschr 156:8–11 Review
17. Stosic-Grujicic S, Stojanovic I, Maksimovic-Ivanic D et al (2008) Macrophage migration inhibitory factor (MIF) is necessary for progression of autoimmune diabetes mellitus. J Cell Physiol 215:665–675
18. Weber UJ, Bock T, Buschard K, Pakkenberg B (1997) Total number and size distribution of motor neurons in the spinal cord of normal and EMC-virus infected mice—a stereological study. J Anat 191:347–353
19. Zhao Y, Shimizu T, Nishihira J et al (2005) Tissue regeneration using macrophage migration inhibitory factor-impregnated gelatin microbeads in cutaneous wounds. Am J Pathol 167:1519–1529

BRAIN RESEARCH 1295 (2009) 192–202

available at www.sciencedirect.com

ScienceDirect

www.elsevier.com/locate/brainres

BRAIN RESEARCH

Research Report

Treatment of rat spinal cord injury with a Rho-kinase inhibitor and bone marrow stromal cell transplantation

Takeo Furuya[a], *Masayuki Hashimoto*[a,*], *Masao Koda*[a], *Akihiko Okawa*[a], *Atsushi Murata*[a], *Kazuhisa Takahashi*[a], *Toshihide Yamashita*[b], *Masashi Yamazaki*[a]

[a]*Department of Orthopaedic Surgery, Chiba University Graduate School of Medicine, 1-8-1 Inohana, Chuo-ku, Chiba 260-8670, Japan*
[b]*Department of Molecular Neuroscience, Osaka University Graduate School of Medicine, 2-2 Yamadaoka Suita 565-0871, Japan*

ARTICLE INFO

Article history:
Accepted 25 July 2009
Available online 3 August 2009

Keywords:
Spinal cord injury
Rho-kinase inhibitor
Fasudil
Bone marrow stromal cell (BMSC)
Cell transplantation

ABSTRACT

In light of reports that the administration of fasudil, a Rho-kinase inhibitor, improved rats locomotor abilities following spinal cord injury, we hypothesized that combining fasudil with another type of therapy, such as stem cell transplantation, might further improve the level of locomotor recovery. Bone marrow stromal cells (BMSCs) are readily available for stem cell therapy. In the present study, we examined whether fasudil combined with BMSC transplantation would produce synergistic effects on recovery. Adult female Sprague–Dawley rats were subjected to spinal cord contusion injury at the T10 vertebral level using an IH impactor (200 Kdyn). Immediately after contusion, they were administrated fasudil intrathecally for 4 weeks. GFP rat-derived BMSCs (2.5×10^6) were injected into the lesion site 14 days after contusion. Locomotor recovery was assessed for 9 weeks with BBB scoring. Sensory tests were conducted at 8 weeks. Biotinylated dextran amine (BDA) was injected into the sensory-motor cortex at 9 weeks. In addition to an untreated control group, the study also included a fasudil-only group and a BMSC-only group in order to compare the effects of combined therapy vs. single-agent therapy. Animals were perfused transcardially 11 weeks after contusion, and histological examinations were performed. The combined therapy group showed statistically better locomotor recovery than the untreated control group at 8 and 9 weeks after contusion. Neither of the two single-agent treatments improved open field locomotor function. Sensory tests showed no statistically significant difference by treatment. Histological and immunohistochemical studies provided some supporting evidence for better locomotor recovery following combined therapy. The average area of the cystic cavity was significantly smaller in the fasudil+BMSC group than in the control group. The number of 5-HT nerve fibers was significantly higher in the fasudil+BMSC group than in the control group on the rostral side of the lesion site. BDA-labeled fibers on the caudal side of the lesion epicenter were observed only in the fasudil+BMSC group. On the other hand, only small numbers of GFP-labeled grafted cells remained 9 weeks after transplantation, and these were mainly localized at the site of injection. Double immunofluorescence studies showed no evidence of differentiation of grafted BMSCs into glial cells or neurons. The

* *Corresponding author*. Fax: +81 43 226 2116.
E-mail address: futre@tg7.so-net.ne.jp (M. Hashimoto).

0006-8993/$ – see front matter
doi:10.1016/j.brainres.2009.07.087

Rho-kinase inhibitor fasudil combined with BMSC transplantation resulted in better locomotor recovery than occurred in the untreated control group. However, the data failed to demonstrate significant synergism from combined therapy compared with the levels of recovery following single-agent treatment.

1. Introduction

Recent efforts to improve treatment for spinal cord injury (SCI) have included stem cell transplantation, drug therapy, and cytokine therapy in various model systems (Ackery et al., 2006; Nishio et al., 2007; Rossignol et al., 2007). However, SCI remains the most devastating type of trauma for patients due to the long lasting disability and the limited response to acute drug administration and efforts at rehabilitation. Although many studies have shown statistically significant recovery following single-agent drug treatment (Baptiste and Fehlings, 2006; Nishio et al., 2007), recovery is generally far from complete. We hypothesized that combined therapies for the appropriate time periods could yield better clinical recovery than a single-agent regimen.

Myelin-associated inhibitors often limit axonal regeneration after SCI (Mueller et al., 2005) as they stimulate intracellular Rho-ROCK kinase activation, leading to neuronal death and growth cone collapse. Targeting Rho-ROCK inhibition is a promising strategy to achieve neuroprotection and axonal regeneration. Fasudil is a ROCK inhibitor, marketed for the treatment of cerebral vasospasm after subarachnoid hemorrhage. Intraperitoneally administered fasudil has significantly improved locomotor recovery after spinal cord injury (Hara et al., 2000). In an experimental spinal cord injury rat study, fasudil significantly improved the BBB score and yielded better outcomes compared with C3 exozyme or Y-27632 (Sung et al., 2003).

Cell transplantation is another approach to neuroprotection and axonal regeneration because it compensates for tissue loss from the SCI. Many cell sources have been used and multiple types of stem cells are now recognized, including the following: ES cells, iPS cells, neural stem cells, adipose tissue-derived stem cells, hematopoietic stem cells, umbilical cord-derived stem cells, and bone marrow-derived stem cells. We previously demonstrated improved locomotion following transplantation of hematopoietic stem cells into mice (Koda et al., 2005; Koshizuka et al., 2004) and bone marrow stromal cell-derived Schwann cells into rats (Kamada et al., 2005).

With respect to stem cells, bone marrow stromal cells (BMSCs) are readily available as they can be collected from the patient and expanded. BMSC transplantation after SCI has resulted in improved locomotor recovery (BBB score) in several previous reports (Chopp et al., 2000; Hofstetter et al., 2002; Ohta et al., 2004; Wu et al., 2003). Some studies have indicated that BMSCs may express trophic factors which improve cell survival (Himes et al., 2006), while others have hypothesized that transplanted BMSCs possess neuroprotective effects (Chen et al., 2005; Chopp and Li, 2002; Neuhuber et al., 2005; Song et al., 2004). Moreover, BMSCs can differentiate to neurons and Schwann cells (Akiyama et al., 2002; Azizi et al., 1998; Chopp and Li, 2002; Deng et al., 2001; Dezawa et al., 2004; Hofstetter et al., 2002; Kim et al., 2002; Kopen et al., 1999; Lee et al., 2004; Sanchez-Ramos et al., 2000; Woodbury et al., 2000; Woodbury et al., 2002). Neurons derived from clonal lines of MSCs have expressed synaptophysin (Woodbury et al., 2002). BMSC-derived neurons have action potentials compatible with those characteristic of functional neurons (Dezawa et al., 2004), suggesting that BMSCs may have the capacity to replace damaged neuronal cells in the spinal cord and form synapses with healthy neurons. On the other hand, transplanted BMSCs do not express neuronal markers (Koda et al., 2005; Lu et al., 2005; Yoshihara et al., 2006), and transplantation does not improve repair or recovery in rats with thoracic contusion injuries (Yoshihara et al., 2006). These discrepancies among spinal cord injury studies will likely require additional studies before they can be resolved.

In the present study, we combined fasudil treatment with BMSC transplantation in a rat spinal cord contusion model. Fasudil administration was started immediately after spinal cord contusion, and BMSCs were injected into the spinal cord 2 weeks later. We assessed the locomotor scale weekly and performed sensory tests 8 weeks after contusion. Histological studies were conducted after 11 weeks to assess tissue preservation and regeneration. In order to detect possible synergistic effects of fasudil and BMSC transplantation, we compared combined (fasudil+BMSC) treatment with single-agent treatments (fasudil alone, BMSCs alone) and with a control group of untreated rats.

2. Results

2.1. *BMSCs showed stem cell-like characteristics in vitro*

Primary cultured BMSCs from GFP-transgenic rats showed fibroblast-like morphology, and their characteristics were maintained over several passages. Because no cell-specific marker for BMSCs has yet been identified, we employed a combination of antibodies in the present study as an alternate approach to detect BMSCs. We based our choice of antibodies on the results of several previous studies (Vimentin and fibronectin, Someya et al., 2008; Nestin, Sauerzweig et al., 2009; CD44, Zhu et al., 2006). Immunocytochemistry showed that primary cultured BMSCs were positive for nestin, fibronectin, vimentin, and CD44 (Fig. 1).

2.2. *Grafted BMSCs survived but did not differentiate into glial cells or neurons in contused spinal cords*

GFP-labeled BMSC grafts survived both in the fasudil+BMSC group and in the BMSC-only group for 9 weeks after transplantation. The majority of the grafted cells remained close to the injection site. The number of donor cells was low in both the fasudil+BMSC group and the BMSC-only group: the mean number of survived transplanted cells was 48.6±44.1 in the Fasudil+BMSC group and 15.4±10.9 in the BMSC-only group. There was no statistically significant difference between these two groups ($p=0.52$). To determine whether grafted rat BMSCs differentiated

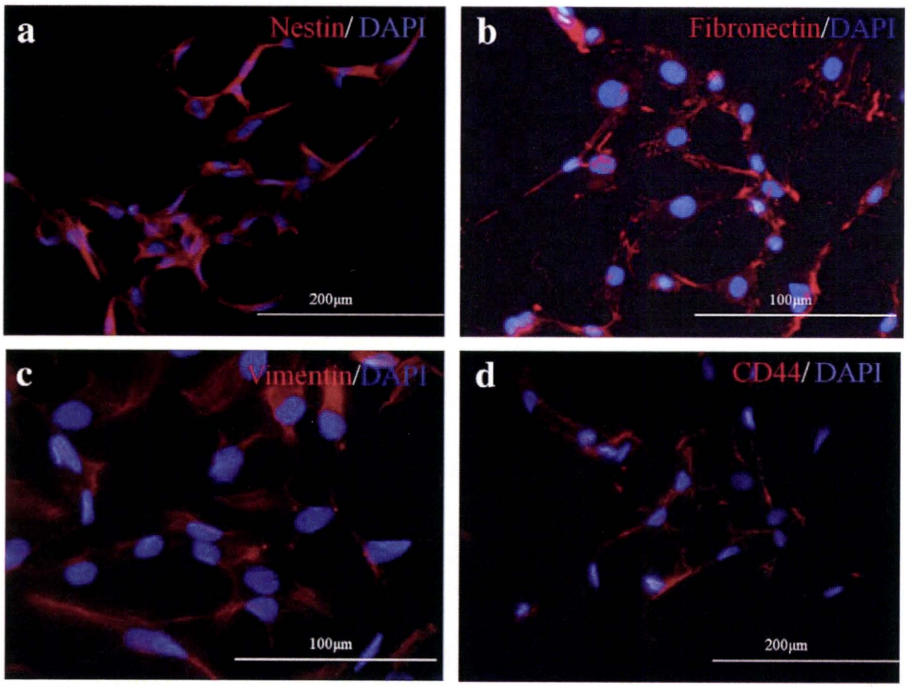

Fig. 1 – In vitro fluorescent immunocytochemical study of GFP-labeled BMSCs. Cells were positive for nestin (a), fibronectin (b), vimentin (c), and CD44 (d), four known markers for BMSC. Original magnification: ×200 for a and d, ×400 for b and c. Scale bar=200 μm for a and d, 100 μm for b and c.

into neural cells, we performed double immunofluorescence of cell-specific markers and GFP (Fig. 2a). GFP-labeled BMSCs did not co-localize with the astrocytic marker GFAP but were clearly separate from GFAP-positive astrocytes (Fig. 2b). GFP-labeled BMSCs also did not co-localize with two other neuronal markers, GSTπ (data not shown) and NeuN (data not shown).

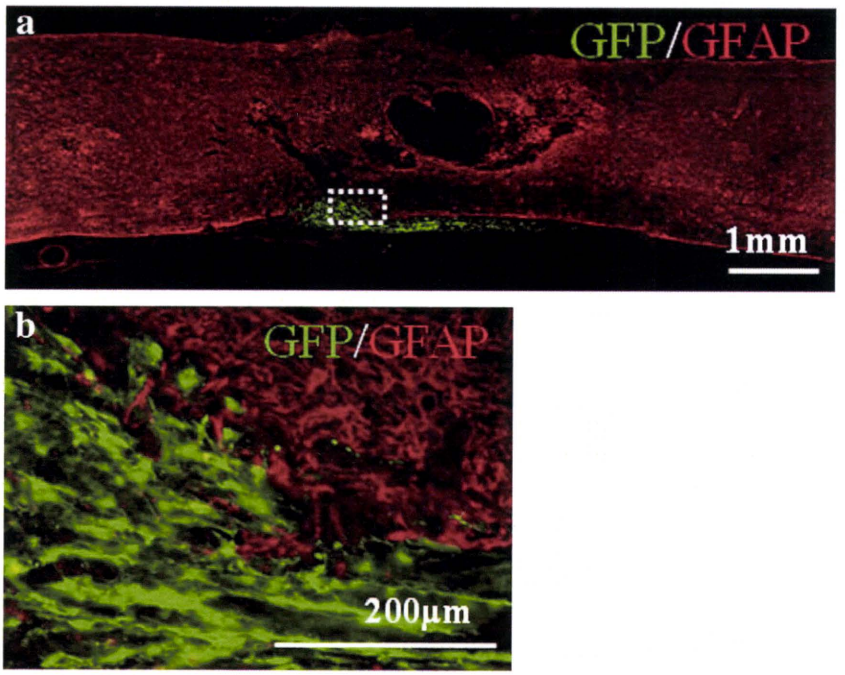

Fig. 2 – Transplanted BMSCs survived *in situ* and showed original markers for BMSC. GFP-labeled BMSCs in representative spinal cord section from the fasudil+BMSC group 9 weeks after transplantation. (a) Representative sagittal spinal cord section demonstrating double immunofluorescence of GFP (green) and GFAP (red). Rostral is to the left. Note that GFP positive cells remained close to the injection site. (b) None of the GFP-labeled cells expressed the astrocytic marker, GFAP. Scale bars=1 mm for a, 200 μm for b.

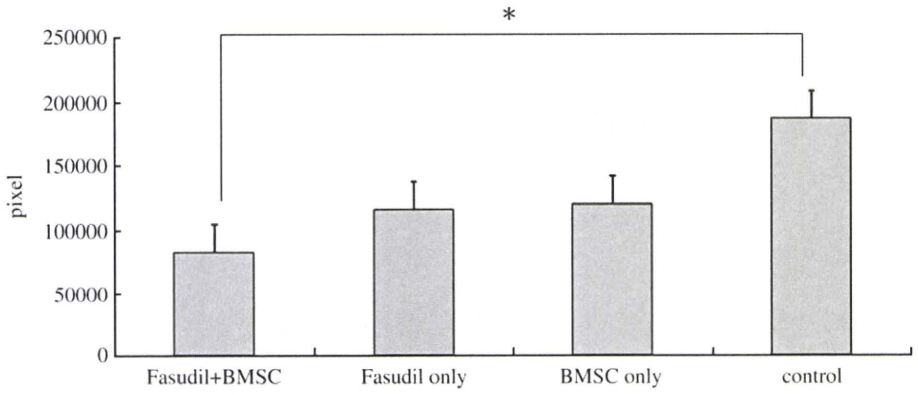

Fig. 3 – Multiple comparisons of cystic cavity formation among four groups. The mean cystic cavity size was smaller for the fasudil+BMSC group than for the control group. *$p<0.05$. The fasudil-only group and BMSC-only group also had smaller cavities than the control group, but these differences were not statistically significant.

2.3. *Combined fasudil infusion and BMSC transplantation reduced the size of the cystic cavity*

To elucidate the efficacy of fasudil treatment and BMSC transplantation for tissue protection or tissue sparing after SCI, we measured the area of the cystic cavity with cresyl violet staining 9 weeks after transplantation. The average area of the cystic cavity was significantly smaller in the fasudil+BMSC group than the control group ($p=0.023$; Fig. 3). The average cystic cavity area did not significantly differ between the other groups.

2.4. *The number of 5-HT nerve fibers was significantly higher following combined therapy with fasudil and BMSC transplantation*

To evaluate axonal survival and regeneration, we counted the number of immunoreactive fibers. We found no statistically significant difference in the number of neurofilament nerve fibers among the four groups (data not shown). The number of 5-HT nerve fibers was significantly higher in the fasudil+BMSC group than in the control group and BMSC-only groups on the rostral side of the lesion site ($p=0.012$, Fig. 4).

2.5. *Combined therapy with fasudil and BMSC transplantation improved CST regeneration/sprouting*

Representative images of traced axons on sagittal sections are shown in Fig. 5. While the groups did not significantly differ from each other in the number of BDA-labeled fibers at the levels of the lesion, BDA-labeled fibers on the caudal side of the lesion epicenter were observed only in the fasudil+BMSC group (Figs. 5a–c). The distance from the tip of the axons to the rostral edge of the scar was measured to assess the degree of axon sprouting; no significant differences among the groups were observed (data not shown).

2.6. *Combined therapy with fasudil and BMSC transplantation enhanced functional recovery in BBB score after SCI*

All groups showed an initial deficit in BBB score following contusion and showed recovery in hind limb function over the next 9 weeks (Fig. 6a). Transplantation surgery did not worsen the behavioral recovery. Hind limb function had recovered significantly in the fasudil +BMSC group at 8 weeks

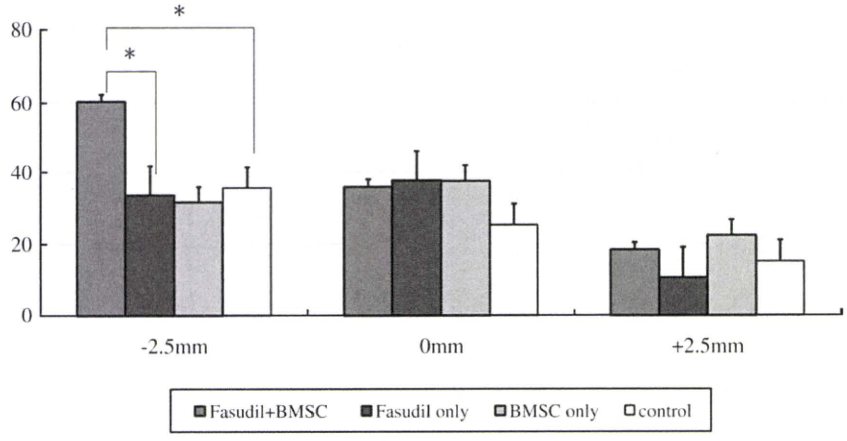

Fig. 4 – Serotonergic fiber counts at rostral, lesion epicenter, and caudal sites of injured spinal cord 11 weeks after SCI. The number of 5-HT nerve fibers in the fasudil+BMSC group was significantly higher than the number in the control and BMSC-only groups on the rostral side of the lesion. No statistically significant differences in 5-HT nerve fiber counts among the groups were observed on the caudal side or at the lesion epicenter. *$p<0.05$.

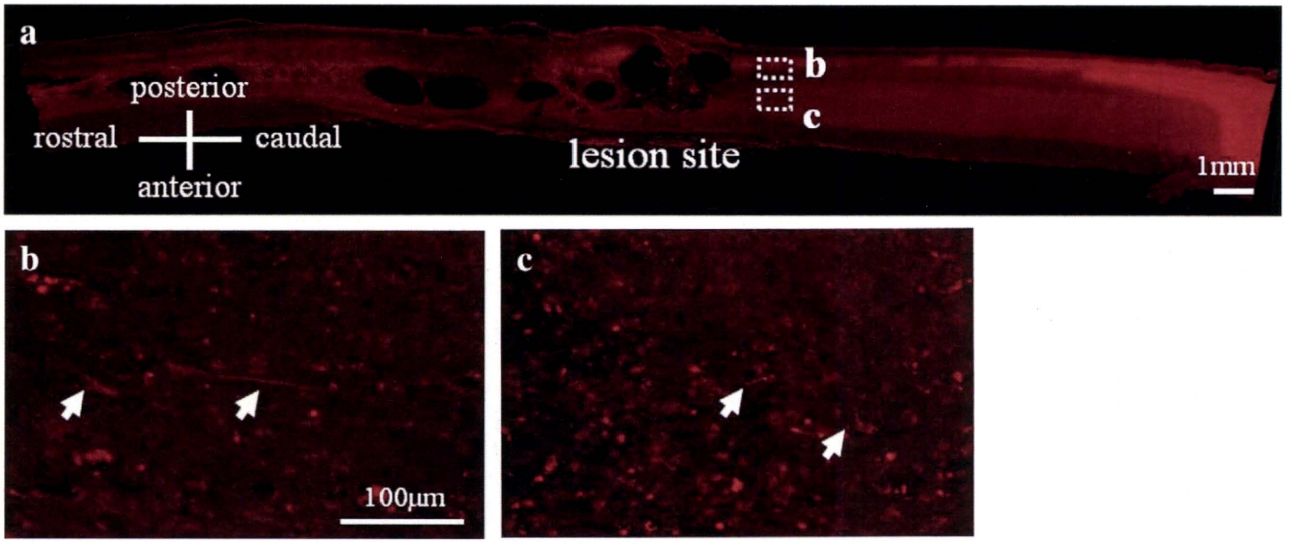

Fig. 5 – Fluorescent histochemistry of corticospinal tract tracing. Representative spinal cord sections of BDA-labeled corticospinal tracts from the fasudil+BMSC group 11 weeks after contusion. (a) Low magnification image of spinal cord sagittal sections. White dot boxes indicate white (b) and gray (c) matter on the caudal sites of the spinal cord lesion. (b, c) Residual or sprouted corticospinal tracts were stained for white (b) and gray (c) matter (arrows) on the caudal sites of the spinal cord lesion. No BDA-labeled corticospinal tracts caudal from the spinal cord lesion are seen in the other groups. Scale bar=1 mm for a, 100 μm for b and c.

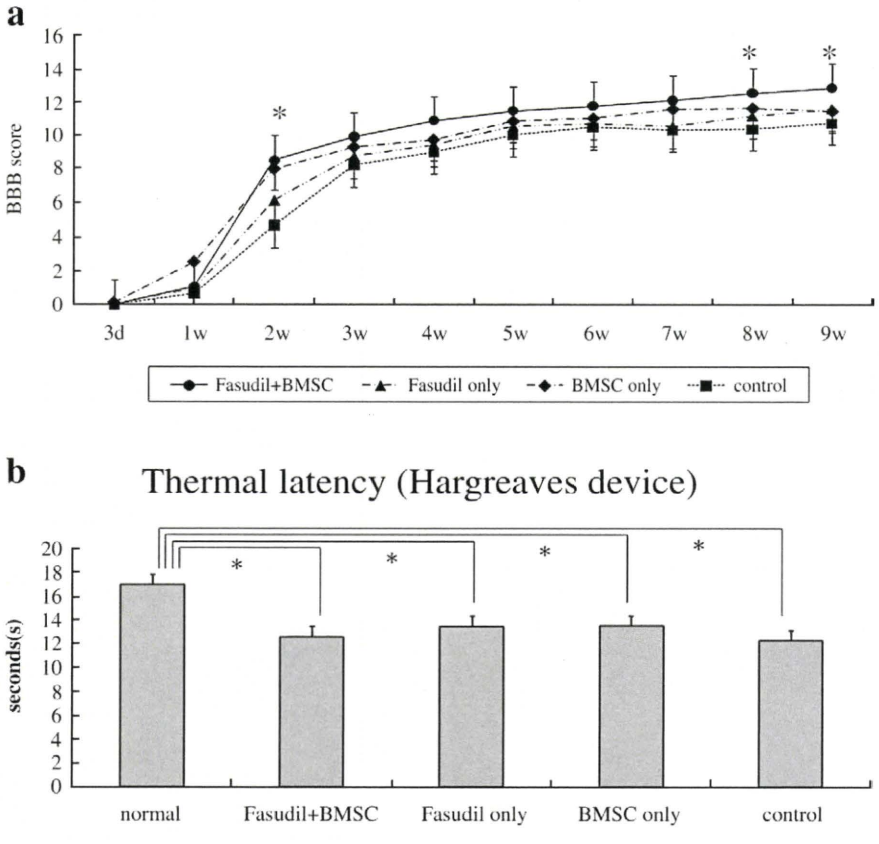

Fig. 6 – Locomotor and sensory recovery from SCI among the four groups. (a) Hind limb function recovered significantly in the fasudil+BMSC group compared with the control group 6 weeks after transplantation. The fasudil-only group and the BMSC-only group also showed better courses of recovery than the control group over time but these improvements did not reach statistical significance. (b) Thermal nociceptive thresholds in rat hind limbs were evaluated using a Hargreaves device. All contused rats showed statistically significant thermal hyperalgesia compared with normal rats. None of the differences in mean thermal latency among the four experimental groups were statistically significant. *$p<0.05$.

after transplantation compared with the control group (p=0.011 at 8 weeks; p=0.010 at 9 weeks). The average BBB score in the fasudil+BMSC group 9 weeks after transplantation reached 12.9±0.4, whereas the average BBB score in the control group was significantly lower (10.8±0.5). The best recovery score in the fasudil+BMSC group was 15. The fasudil-only group and the BMSC-only group showed better courses of recovery than the control group over time but these improvements did not reach statistical significance. These results demonstrate that fasudil treatment combined with BMSC transplantation promoted recovery of open field locomotor function after contusion of the spinal cord in rats. Neither single treatment with fasudil nor transplantation of BMSCs alone in this study protocol improved open field locomotor function.

2.7. *Fasudil and/or BMSC transplantation did not increase abnormal neurogenic pain*

Analysis of normal rats with a Hargreaves device revealed a mean thermal latency of 17.0±0.3 s (Fig. 6b) compared with mean values of 12.6±0.7 s in the fasudil+BMSC group, 13.5±1.3 s in the fasudil-only group, 13.6±1.1 s in the BMSC-only group, and 12.3±1.1 s in the control group 8 weeks after contusion. Thus, while all contused rats showed significant thermal hyperalgesia compared with normal rats (p=0.00087), none of the differences in mean thermal latency among the four experimental groups were statistically significant.

Mechanical thresholds using a dynamic plantar aesthesiometer showed a mean of 32.6±1.2 g in normal rats, decreasing to 32.2±2.1 g in the fasudil+BMSC group, 31.5±3.7 g in the fasudil-only group, 32.0±2.5 g in the BMSC-only group, and 31.2±5.8 g in the control group 8 weeks after contusion. All contused rats showed more mechanical allodynia compared to normal rats; however, no statistically significant increase in allodynia as a function of treatment was observed (data not shown). These two studies indicate that fasudil and/or BMSC transplantation did not increase abnormal neurogenic pain.

3. Discussion

In our study of rats with spinal cord contusion injury, we found that combined therapy with fasudil infusion and BMSC transplantation improved functional recovery and reduced cystic cavity size compared with controls.

3.1. *Fasudil infusion*

Rho and Rho-kinase exert their effects through regulation of the actin–myosin network (Amano et al., 2000; Dickson, 2001). Rho-kinase stimulates actin–myosin contractility by phosphorylating the myosin light chain and inhibiting myosin phosphatase. Following SCI, scar tissue containing myelin-derived inhibitors and chondroitin sulfate proteoglycans (CSPG) inhibits neurite outgrowth or induces growth cone collapse by activating the Rho/Rho-kinase signaling pathway (Mueller et al., 2005). The effects of myelin-derived inhibitors and CSPG are abolished when Rho-kinase is inhibited (Kubo and Yamashita, 2007; Monnier et al., 2003). Fasudil or Rho-kinase inhibition also has neuroprotective effects, as evidenced by studies showing that fasudil infusion reduced MPO activity in rats (Hara et al., 2000) and hindered ischemia-induced delayed neuronal death in gerbils (Satoh et al., 2007). Another study reported that fasudil application reversed Rho activation and reduced the number of TUNEL-labeled cells by approximately 50% in mice and rats with SCI (Dubreuil et al., 2003).

We hypothesized that fasudil infusion overcomes myelin-derived inhibition after spinal cord injury by inhibiting Rho-ROCK-kinase. We also hypothesized that a longer duration of fasudil administration would improve axonal regeneration or neuronal survival, which we tested in the present study by continuing fasudil administration for four weeks. However, our study found that the fasudil-only group did not show a statistically significant difference in locomotor recovery compared with the control group. One possible explanation for this observation is that after a certain point, further fasudil infusion becomes counterproductive and increases myelin inhibition, thereby slowing axonal regeneration for locomotor recovery. Support for this explanation comes from a recent study which discovered that another Rho-kinase inhibitor, Y27632, increased CSPG (Chan et al., 2007).

The extent of penetration of fasudil into the spinal cord is a critical concern. One report demonstrated that intraperitoneal administration of fasudil reduced MPO activity in injured spinal cords (Hara et al., 2000). Another study found that intrathecal fasudil treatment reduced thermal hyperalgesia in post-sciatic nerve ligation rats (Shiokawa et al., 2007). These two studies thus represent evidence that fasudil does permeate into the spinal cord.

3.2. *BMSC transplantation*

BMSC transplantation is a potential therapy for central nervous system (CNS) diseases because BMSCs secrete a variety of growth factors and cytokines that could contribute to the repair of CNS injuries. Following stimulation of TNF-alpha, ELISA assay findings indicate that BMSCs increase the release of IL-6, MCP-1, and BDNF (Himes et al., 2006). BMSCs trigger the endogenous survival signaling pathway Erk1/2 and also trigger Akt phosphorylation in neurons (Isele et al., 2007). BMSCs have the potential to support the survival of neurons in the marginal region of SCI (Yano et al., 2006).

BMSCs are also capable of differentiating into a variety of tissues. Some studies have suggested that BMSCs can differentiate into cells with neural phenotypes (Chopp et al., 2000). Others have reported that the apparent acquisition of a neuronal phenotype by BMSCs results from cell fusion or cell phagocytosis (Alvarez-Dolado et al., 2003; Hess et al., 2004; Terada et al., 2002; Ying et al., 2002). In an earlier experiment, we transplanted BMSC-derived Schwann cells to treat rat spinal cord defects and identified significantly improved locomotor recovery compared with controls (Kamada et al., 2005). Some studies by other researchers have reported significant functional recovery after transplanting BMSCs (Chopp et al., 2000; Hofstetter et al., 2002; Ohta et al., 2004; Wu et al., 2003), while others have

identified only modest or inconsistent recovery (Himes et al., 2006; Lu et al., 2005; Neuhuber et al., 2005; Yoshihara et al., 2006). In the present study, our assessments of behavior and histology following BMSC transplant-alone did not detect significantly different locomotor recovery compared with the control group.

Lack of a significant therapeutic effect following BMSC transplantation alone might be attributable to the timing of the transplantation. We chose to perform cell transplantation 2 weeks after SCI because some interval for cell culturing is required in actual clinical autograft transplantation. However, our treatment timing might have hindered efficacy, as evidenced by the low number of surviving cells. Furthermore, if our aim were to enhance host neural survival by BMSC transplantation, this 2-week delay would have caused the intervention to be too late to save neurons from consecutive death after SCI because neural death after spinal cord injury often happens within one day (Liu et al., 1997).

Another possible reason for the poor response was the site of the transplantation. We injected BMSCs into rostral and caudal sites to facilitate migration of BMSCs and re-myelination of regenerative fibers. However, histological examination found that residual BMSCs were scarce and that they did not migrate as we had expected they would. Thus, transplanting BMSCs directly into the site of injury might yield better outcomes.

3.3. *Combined therapy*

In our study, fasudil+BMSC therapy increased 5-HT-positive fibers on the rostral side of the lesion, enhanced CST regeneration and/or sprouting, and significantly reduced mean cystic cavity size compared with the control group. These histological results were consistent with a significant improvement in locomotor activity.

As we discussed previously, increased fasudil infusion beyond a certain point might become counterproductive and increase myelin inhibition. One study found that BMSCs stimulated neurite outgrowth over CSPG, myelin-associated glycoprotein, and Nogo-A in vitro (Wright et al., 2007). Thus, the sprouting of CST and serotonergic fibers observed under combined treatment might reflect the effect of BMSC transplantation, which can stimulate neurite outgrowth over inhibitory proteins. On the other hand, another study revealed that Rho-pathway inhibition after cervical dorsal rhizotomy in rats increased the density of serotonergic fibers in the dorsal horn (Ramer et al., 2004). Correspondingly in the present study, fasudil, a Rho-pathway inhibitor, likewise may have taken part in the regeneration of serotonergic fibers observed in the fasudil+BMSC group. Overall, Fasudil-induced Rho-kinase inhibition and BMSC transplantation each appear to provide some degree of neuroprotection against neuronal death (Chen et al., 2005; Chopp and Li, 2002; Dubreuil et al., 2003; Neuhuber et al., 2005; Satoh et al., 2007; Song et al., 2004).

In the present study, the mean cystic cavity area was significantly smaller in the fasudil+BMSC group than in the control group. Since neither fasudil alone nor BMSCs alone significantly changed the size of the cystic cavity compared with the control group, these findings together suggest it was the combination of fasudil infusion and BMSC transplantation that produced reductions in cystic areas that neither agent alone could achieve. These histological findings also suggest that fasudil and BMSC transplantation in combination had anti-inflammatory activity which suppressed local inflammatory reactions from SCI. Several published studies have also reported that fasudil exhibited anti-inflammatory activity. Intraperitoneal administration of fasudil in rats with collagen-induced arthritis significantly reduced synovial inflammation and ROCK activity (He et al., 2008). In vitro treatment with fasudil or Y27632 decreased production of tumor necrosis factor alpha (TNFalpha), interleukin-1beta (IL-1beta), and IL-6 by synovial membrane cells, peripheral blood mononuclear cells, and fibroblast-like synoviocytes from patients with active rheumatoid arthritis (He et al., 2008).

Because the number of residual transplanted BMSCs was low in all BMSC transplantation groups 9 weeks after transplantation, improved locomotor recovery is unlikely to have resulted from BMSCs alone. Also, the BMSC-only group did not show significantly greater recovery than the level of recovery in the control group. Thus, it appears that better locomotor recovery results from the combination of fasudil and BMSC, the effectiveness of which might arise from BMSCs acting to reverse the putative toxicity of high total dosage fasudil treatment.

The BBB score for combined therapy reached 12.9 while the control group BBB score reached 10.8. Although rats in both groups could perform weight-bearing plantar stepping, only the rats in the combined treatment group had coordination of fore limbs and hind limbs. These results indicate that combined therapy could enhance recovery of a central pattern generator.

In summary, combined therapy showed better locomotor recovery compared with controls, and histological studies of cavity volume and serotonergic fiber counts confirmed the locomotor results. Future studies are required to identify the effect of combined fasudil infusion and BMSC transplantation to clarify any potential clinical application to damaged spinal cords in humans.

4. Experimental procedures

4.1. *Bone marrow stromal cell culture*

Bone marrow stromal cells (BMSCs) were collected from the femurs and tibias of 8-week-old female GFP transgenic Sprague–Dawley rats (SLC, Hamamatsu, Japan). Briefly, animals received an overdose of pentobarbital to induce deep anesthesia and were then decapitated. Bone marrow was flushed with PBS and centrifuged at 1500 rpm for 5 min. Cells were plated in α-MEM (Sigma, St. Louis, MO) plus 10% fetal bovine serum supplemented with 100 U/mL penicillin G and 100 μg/mL streptomycin (Molecular Probes, Eugene, OR) and then incubated at 37 °C in 5.0% CO2. After non-adherent cells were removed just before confluency, adherent cells were detached using 0.25% trypsin with EDTA, centrifuged, and re-plated as BMSCs. BMSCs were used for transplantation and in vitro induction experiments between passages four to eight.

To characterize the BMSCs in vitro, we performed immunocytochemistry using the following primary antibodies: anti-

vimentin mouse monoclonal antibody (1:200; Dako Cytomation, Copenhagen, Denmark), anti-fibronectin mouse monoclonal antibody (1:400; Chemicon International, Temecula, CA), anti-nestin rabbit polyclonal antibody (1:400; Chemicon International), and anti-CD44 mouse monoclonal antibody (1:400; Serotec Ltd., Oxford, England). Cell nuclei were stained with DAPI (1:1000, Molecular Probes). We omitted the primary antibodies for negative controls. After reacting with primary antibodies, sections were incubated with appropriate secondary antibodies.

4.2. *Animal surgery*

For experimental spinal cord injury (SCI), we used a total of 37 female Sprague–Dawley rats aged 8–10 weeks (weight 174–236 g; SLC). Fig. 7 shows the time line of the present study. Rats were anesthetized with 1.6% halothane in 0.5 L/min oxygen. Laminectomy was performed at the T9–T10 levels, and contusion injury was introduced using the Infinite Horizon impactor (IH impactor, 200 Kdyn, Precision Systems and Instrumentation, Lexington, NY). Immediately after SCI, a thin silicone tube was inserted into the subarachnoid space at the laminectomized L1 level using a surgical microscope. The tube was connected to an Alzet osmotic mini pump (model 2004; Alza, Paolo Alto, CA) containing 30 μg/μL fasudil (Asahi Kasei Inc., Tokyo, Japan) in saline. The infusion rate was 6.0 μL/day resulting in the infusion of 180 μg/day of fasudil. The infusion was continued for 4 weeks, resulting in a total fasudil infusion of approximately 5.04 mg /animal. Rats were group-housed in the animal facility and maintained under constant temperature and humidity conditions. Food and water were provided *ad libitum*. Manual bladder expression was performed twice a day until recovery of the bladder reflex. All animals were given antibiotics (500 μL/day; Bactramin, Chuugai Pharmaceutical, Tokyo, Japan) by subcutaneous administration once a day for 3 days.

Fourteen days after injury, the injured site was re-exposed and the same volume of BMSCs or saline was injected by micro-glass pipette needle attached to a 10 μL Hamilton syringe (Hamilton Company, Reno, NV). The injection was made at several depths during drawback in each injection, and the needle was left in the spinal cord for one additional minute following injection in order to minimize reflux. The injection sites were located at 4 mm intervals on the rostral and caudal edges of the lesion site (5.0×10^5 cells/μL, 2. 5 μL each, 2.5×10^6 cells/total). All animals, including control groups, were immunosuppressed with cyclosporine A (Sandimmun, Novartis, Basel, Switzerland) for the remaining experimental period (20 mg/kg on Monday and Wednesday, 40 mg/kg on Friday) (Wennersten et al., 2004). None of the animals showed abnormal behavior. All the experimental procedures were performed in compliance with the guidelines established by the Animal Care and Use Committee of Chiba University.

4.3. *Experimental groups*

The rats were randomly divided into four groups (Table 1). The fasudil+BMSC group ($n=10$) received fasudil by Alzet osmotic mini pump, as explained above and BMSCs were transplanted into the spinal cord. The fasudil-only group ($n=8$) received fasudil by Alzet pump and saline injection into the spinal cord. The BMSC-only group ($n=9$) received saline by Alzet pump and BMSC transplantation into the spinal cord. The control group ($n=10$) received saline via Alzet pump and saline injection into the spinal cord. One animal of BMSC-only group was sacrificed to make sure that BMSC was survived three weeks after BMSCs transplantation.

4.4. *Assessments of sensory motor functions*

4.4.1. *BBB open field locomotor test*

Hind limb function was assessed in an open field (100×60 cm plastic pool) using the BBB open field locomotor test (Basso et al., 1995). Measurements were performed 3 days after contusion injury and weekly thereafter for 9 weeks. Tests were videotaped and scored by two trained observers who were unaware of the treatment group.

4.4.2. *Sensory tests*

Thermal nociceptive thresholds in rat hind limbs were evaluated using a Hargreaves device (Ugo Basile, Varese, Italy). The rat was deposited into individual transparent acrylic boxes with the floor maintained at 28 °C. A heat stimulus (150 mcal/s/cm^2) was delivered using a 0.5 cm diameter radiant heat source positioned under the plantar surface of the hind limb. The heat source was placed alternately under each hind limb to avoid anticipation by the animal. A cutoff time of 22 s was used, as it had been ascertained that no tissue damage would result within this

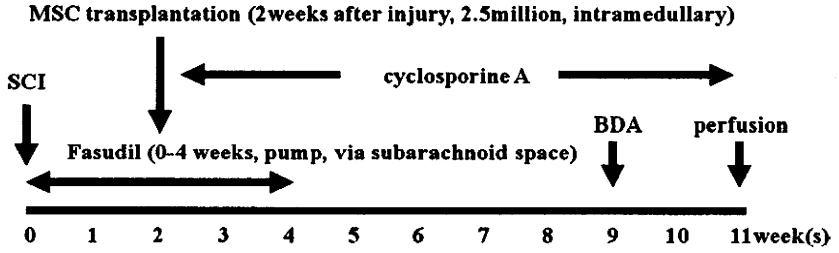

Fig. 7 – Experimental protocol. Immediately after SCI (T9–T10 levels; IH impactor, 200 Kdyn), fasudil was administered by an Alzet mini-osmotic pump via the subarachnoid space into the injury site for four weeks. Two weeks after contusion, 2.5×10^6 GFP-tagged BMSCs were transplanted into the lesion site. All animals were immunosuppressed with cyclosporin A for the remaining experimental period. BDA was injected into the sensory-motor cortex 9 weeks after contusion. Animals were perfused transcardially, and histological examination was performed eleven weeks after contusion.

Table 1 - Experimental groups.

Groups	Number of rats	Treatment	
		Infusion by Alzet pump	Transplantation
Fasudil+BMSC group	10	Fasudil	BMSC
Fasudil-only group	8	Fasudil	Saline
BMSC-only group	9	Saline	BMSC
Control group	10	Saline	Saline

The rats were randomly divided into four groups. The fasudil +BMSC group ($n=10$) received fasudil administration by Alzet osmotic mini pump and BMSC transplantation into the spinal cord. The fasudil-only group ($n=8$) received fasudil administration by Alzet pump and saline injection into the spinal cord. The BMSC-only group ($n=9$) received saline administration by Alzet pump and BMSC transplantation into the spinal cord. The control group ($n=10$) received saline administration by Alzet pump and saline injection into the spinal cord.

time period. The withdrawal threshold was calculated as the average of six consecutive tests.

Mechanical withdrawal thresholds in rat hind limbs were tested using a Dynamic Plantar Aesthesiometer (Ugo Basile), in which a mechanical stimulus was applied via an actuator filament (0.5 mm diameter), which under computer control applies a linear ramp 5.0 g/s to the plantar surface of the hind limb. The withdrawal threshold was calculated as the average of six consecutive tests. Both tests were performed 8 weeks after contusion. For comparison with baseline, we also performed both tests with normal rats ($n=31$).

4.5. *Anterograde labeling of corticospinal tracts with BDA, immunohistochemical, and histological assessment*

Nine weeks after contusion, the corticospinal tract (CST) was hemilaterally traced under halothane anesthesia with 2.0 μL biotinylated dextran amine (BDA, molecular weight: 10,000, 10% in 0.01 M PBS, Molecular Probes). A micro-glass pipette needle attached to a 2 μL Hamilton syringe was stereotaxically guided, and BDA was slowly injected into four sites in the sensorimotor cortex for the hind limb at a depth of 1 mm. The needle was left for an additional 1 min following each injection to minimize reflux.

Animals were subjected to trans-cardiac perfusion with 4% paraformaldehyde in PBS (pH 7.4) for 14 days after BDA injection. At the conclusion of the BDA infusion period (11 weeks after contusion), the spinal cords were dissected and immersed overnight in 4% paraformaldehyde, then stored in 20% sucrose in PBS. The spinal cords were cut into 20 mm lengths (10 mm rostral and 10 mm caudal from the lesion site) and embedded in OCT compound (Tissue Tek, Sakura Finetechnical, Tokyo, Japan). These blocks were sectioned in the sagittal plane (section thickness=25 μm) using a cryostat. We mounted a set of serial sections on a total of eight poly-L-lysine-coated slides (Matsunami, Tokyo, Japan) for each animal. Each slide contained six sliced sections at 200 μm intervals, and the sections for each slide were offset by 25 μm from the previous slide in the set. By this method, we were able to cover approximately 1200 μm of the lesion at 25 μm intervals in these eight slides. We processed the slides for histological or immunohistochemical staining.

To evaluate lesion size, one slide from one animal was stained with cresyl violet. The three slices showing the greatest damage were selected from one slide, and cavity size was determined with Photoshop 5.5 software (Adobe, San Jose, CA). Mean lesion size values for each group were calculated using these three lesions size values for each animal, and mean size comparisons were performed among the four groups.

In order to identify cell populations and characterize the cellular response, sections were immunolabeled with one or more antibodies. Anti-green fluorescent protein (GFP, rabbit polyclonal antibody, 1: 1600, Molecular Probes) was used to identify grafted rat BMSCs. The number of surviving transplanted cells and the localization of the cells were evaluated. Double immunohistochemical staining was performed with GFP plus either mouse anti-glial fibrillary acidic protein (GFAP, 1:400, Sigma, St. Louis, MO) or mouse anti-GSTπ (1:400, BD Pharmingen, Franklin Lakes, NJ), or mouse anti-NeuN (1:400; Chemicon) to evaluate transdifferentiation of BMSCs into astrocytes, oligodendrocytes, and neurons, respectively. After reacting with primary antibodies, the sections were incubated with Alexa Fluor 488-conjugated anti-mouse or anti-rabbit IgG (Molecular Probes) and with Alexa Fluor 594-conjugated anti-mouse or anti-rabbit IgG (Molecular Probes).

To evaluate residual and regenerative fibers, rabbit anti-neurofilament polyclonal antibody (1:800, Sigma) and rabbit anti-serotonin (5-HydroxyTryptamine, 5-HT) polyclonal antibody (1:5000, Sigma) were used for pan-nerve fibers. After reacting with primary antibodies, the sections were incubated with Alexa Fluor 488-conjugated anti-rabbit IgG (Molecular Probes) to detect positive signals. The numbers of immunoreactive fibers that traversed the virtual lines perpendicular to the central axis of the grafts were counted at three locations: the lesion site, 2.5 mm rostral from the lesion site, and 2.5 mm caudal from the lesion site.

For anterograde labeling of CSTs with BDA, sections were incubated with Alexa Fluor 594-conjugated streptavidin (1:800; Molecular Probes). The distance from the end of the labeled axons to the edge of the lesion site and the number of CST axons at the lesion site were measured.

The fluorescent signals were observed by fluorescence microscopy, ECLIPSE E600 (Nikon, Tokyo, Japan), and DP71 (Olympus, Tokyo, Japan). To maintain blinding in this histological study, observers were kept unaware of treatment groups.

4.6. *Statistical analysis*

Data were evaluated by multiple comparisons between groups. For histological studies, one-way ANOVA followed by the Bonferroni/Dunn *post hoc* test was used. For the 9-week locomotor scale, repeated-measures ANOVA followed by the Turkey-Kramer *post hoc* test was used. For fractional BBB score at each time point, one-way ANOVA followed by the Turkey-Kramer *post hoc* test was used. Data are presented as mean values±SEM. Differences were considered statistically significant at $^{*}p<0.05$.

Acknowledgments

Fasudil was kindly provided by Asahi Kasei Corporation (Tokyo, Japan). This research was supported by grant-in-aid for Japanese scientific research grant 19591715.

REFERENCES

Ackery, A., Robins, S., Fehlings, M.G., 2006. Inhibition of Fas-mediated apoptosis through administration of soluble Fas receptor improves functional outcome and reduces posttraumatic axonal degeneration after acute spinal cord injury. J. Neurotrauma 23, 604–616.

Akiyama, Y., Radtke, C., Kocsis, J.D., 2002. Remyelination of the rat spinal cord by transplantation of identified bone marrow stromal cells. J. Neurosci. 22, 6623–6630.

Alvarez-Dolado, M., Pardal, R., Garcia-Verdugo, J.M., Fike, J.R., Lee, H.O., Pfeffer, K., Lois, C., Morrison, S.J., Alvarez-Buylla, A., 2003. Fusion of bone-marrow-derived cells with Purkinje neurons, cardiomyocytes and hepatocytes. Nature 425, 968–973.

Amano, M., Fukata, Y., Kaibuchi, K., 2000. Regulation and functions of Rho associated kinase. Exp. Cell Res. 261, 44–51.

Azizi, S.A., Stokes, D., Augelli, B.J., DiGirolamo, C., Prockop, D.J., 1998. Engraftment and migration of human bone marrow stromal cells implanted in the brains of albino rats- Similarities to astrocyte grafts. Proc. Natl. Acad. Sci. U. S. A. 95, 3908–3913.

Baptiste, D.C., Fehlings, M.G., 2006. Pharmacological approaches to repair the injured spinal cord. J. Neurotrauma 23, 318–334.

Basso, D.M., Beattie, M.S., Bresnahan, J.C., 1995. A sensitive and reliable locomotor rating scale for open field testing in rats. J. Neurotrauma 12, 1–21.

Chan, C.C., Wong, A.K., Liu, J., Steeves, J.D., Tetzlaff, W., 2007. ROCK inhibition with Y27632 activates astrocytes and increases their expression of neurite growth-inhibitory chondroitin sulfate proteoglycans. Glia 55, 369–384.

Chen, Q., Long, Y., Yuan, X., Zou, L., Sun, J., Chen, S., Perez-Polo, J.R., Yang, K., 2005. Protective effects of bone marrow stromal cell transplantation in injured rodent brain: synthesis of neurotrophic factors. J. Neurosci. Res. 80, 611–619.

Chopp, M., Zhang, X.H., Li, Y., Wang, L., Chen, J., Lu, D., Lu, M., Rosenblum, M., 2000. Spinal cord injury in rat: treatment with bone marrow stromal cell transplantation. Neuroreport 11, 3001–3005.

Chopp, M., Li, Y., 2002. Treatment of neural injury with marrow stromal cells. Lancet Neurol. 1, 92–100 Review.

Deng, W., Obrocka, M., Fischer, I., Prockop, D.J., 2001. In vitro differentiation of human stromal cells into early progenitors of neural cells by conditions that increase intracellular cyclic AMP. Biol. Biophys. Res. Commun. 282, 148–152.

Dezawa, M., Kanno, H., Hoshino, M., Cho, H., Matsumoto, N., Itokazu, Y., Tajima, N., Yamada, H., Sawada, H., Ishikawa, H., Mimura, T., Kitada, M., Suzuki, Y., Ide, C., 2004. Specific induction of neuronal cells from bone marrow stromal cells and application for autologous transplantation. J. Clin. Invest. 113, 1701–1710.

Dickson, B.J., 2001. Rho GTPases in growth cone guidance. Curr. Opin. Neurobiol. 11, 103–110.

Dubreuil, C.I., Winton, M.J., McKerracher, L., 2003. Rho activation patterns after spinal cord injury and the role of activated Rho in apoptosis in the central nervous system. J. Cell Biol. 162, 233–243.

Hara, M., Takayasu, M., Watanabe, K., Noda, A., Takagi, T., Suzuki, Y., Yoshida, J., 2000. Protein kinase inhibition by fasudil hydrochloride promotes neurological recovery after spinal cord injury in rats. J. Neurosurg. 93 (1 Suppl.), 94–101.

He, Y, Xu, H, Liang, L, Zhan, Z, Yang, X, Yu, X, Ye, Y, Sun, L., 2008. Antiinflammatory effect of Rho kinase blockade via inhibition of NF-kappaB activation in rheumatoid arthritis. Arthritis Rheum. 58, 3366–3376.

Hess, D.C., Abe, T., Hill, W.D., Studdard, A.M., Carothers, J., Masuya, M., Fleming, P.A., Drake, C.J., Ogawa, M., 2004. Hematopoietic origin of microglial and preivascular cells in brain. Exp. Neurol. 186, 134–144.

Himes, B.T., Neuhuber, B., Coleman, C., Kushner, R., Swanger, S.A., Kopen, G.C., Wagner, J., Shumsky, J.S., Fischer, I., 2006. Recovery of function following grafting of human bone marrow-derived stromal cells into the injured spinal cord. Neurorehabilitation Neural. Repair 20, 278–296.

Hofstetter, C.P., Schwarz, E.J., Hess, D., Widenfalk, J., El Manira, A., Prockop, D.J., Olson, L., 2002. Marrow stromal cells from guiding strands in the injured spinal cord and promote recovery. Proc. Natl. Acad. Sci. U. S. A. 99, 2199–2204.

Isele, N.B., Lee, H.S., Landshamer, S., Straube, A., Padovan, C.S., Plesnila, N., Culmsee, C., 2007. Bone marrow stromal cells mediate protection through stimulation of PI3-K/Akt and MAPK signaling in neurons. Neurochem. Int. 50, 243–250.

Kamada, T., Koda, M., Dezawa, M., Yoshinaga, K., Hashimoto, M., Koshizuka, S., Nishio, Y., Moriya, H., Yamazaki, M., 2005. Transplantation of bone marrow stromal cell-derived Schwann cells promotes axonal regeneration and functional recovery after complete transection of adult rat spinal cord. J. Neuropathol. Exp. Neurol. 64, 37–45.

Kim, B.J., Seo, J.H., Bubien, J.K., Oh, Y.S., 2002. Differentiation of adult bone marrow stem cells into neuroprogenitor cells in vitro. Neuroreport 13, 1185–1188.

Koda, M., Okada, S., Nakayama, T., Koshizuka, S., Kamada, T., Nishio, Y., Someya, Y., Yoshinaga, K., Okawa, A., Moriya, H., Yamazaki, M., 2005. Hematopoietic stem cell and marrow stromal cell for spinal cord injury in mice. Neuroreport 16, 1763–1767.

Kopen, G.C., Prockop, D.J., Phinney, D.G., 1999. Marrow stromal cells migrate throughout forebrain and cerebellum, and they differentiate into astrocytes after injection into neonatal mouse brains. Proc. Natl. Acad. Sci. U. S. A. 96, 10711–10716.

Koshizuka, S., Okada, S., Okawa, A., Koda, M., Murasawa, M., Hashimoto, M., Kamada, T., Yoshinaga, K., Murakami, M., Moriya, H., Yamazaki, M., 2004. Transplanted hematopoietic stem cells from bone marrow differentiate into neural lineage cells and promote functional recovery after spinal cord injury in mice. J. Neuropathol. Exp. Neurol. 63, 64–72.

Kubo, T., Yamashita, T., 2007. Rho-ROCK inhibitors for the treatment of CNS injury. Recent Patents CNS Drug Discov. 2, 173–179.

Lee, J.B., Kuroda, S., Shichinohe, H., Yano, S., Kobayashi, H., Hida, K., Iwasaki, Y., 2004. A pre-clinical assessment model of rat autogeneic bone marrow stromal cell transplantation into the central nervous system. Brain Res. Brain Res. Protoc. 14, 37–44.

Liu, X.Z., Xu, X.M., Hu, R., Du, C., Zhang, S.X., McDonald, J.W., Dong, H.X., Wu, Y.J., Fan, G.S., Jacquin, M.F., Hsu, C.Y., Choi, D.W., 1997. Neuronal and glial apoptosis after traumatic spinal cord injury. J. Neurosci. 17, 5395–5406.

Lu, P., Jones, L.L., Tuszynski, M.H., 2005. BDNF-expressing marrow stromal cells support extensive axonal growth at sites of spinal cord injury. Exp. Neurol. 191, 344–360.

Monnier, P.P., Sierra, A., Schwab, J.M., Henke-Fahle, S., Mueller, B.K., 2003. The Rho/ROCK pathway mediates neurite growth-inhibitory activity associated with the chondroitin sulfate proteoglycans of the CNS glial scar. Mol. Cell. Neurosci. 22, 319–330.

Mueller, B.K., Mack, H., Teusch, N., 2005. Rho kinase, a promising drug target for neurological disorders. Nat. Rev. Drug Discov. 4, 387–398.

Neuhuber, B., Timothy Himes, B., Shumsky, J.S., Gallo, G., Fischer, I., 2005. Axon growth and recovery of function supported by

human bone marrow stromal cells in the injured spinal cord exhibit donor variations. Brain Res. 1035, 73–85.
Nishio, Y., Koda, M., Kamada, T., Someya, Y., Kadota, R., Mannoji, C., Miyashita, T., Okada, S., Okawa, A., Moriya, H., Yamazaki, M., 2007. Granulocyte colony-stimulating factor attenuates neuronal death and promotes functional recovery after spinal cord injury in mice. J. Neuropathol. Exp. Neurol. 66, 724–731.
Ohta, M., Suzuki, Y., Noda, T., Ejiri, Y., Dezawa, M., Kataoka, K., Chou, H., Ishikawa, N., Matsumoto, N., Iwashita, Y., Mizuta, E., Kuno, S., Ide, C., 2004. Bone marrow stromal cells infused into the cerebrospinal fluid promote functional recovery of the injured rat spinal cord with reduced cavity formation. Exp. Neurol. 187, 266–278.
Ramer, LM, Borisoff, JF, Ramer, MS., 2004. Rho-kinase inhibition enhances axonal plasticity and attenuates cold hyperalgesia after dorsal rhizotomy. J Neurosci. 24, 10796–10805.
Rossignol, S., Schwab, M., Schwartz, M., Fehlings, M.G., 2007. Spinal cord injury: time to move? J. Neurosci. 27, 11782–11792 Review.
Sanchez-Ramos, J., Song, S., Cardozo-Pelaez, F., Hazzi, C., Stedeford, T., Willing, A., Freeman, T.B., Saporta, S., Janssen, W., Patel, N., Cooper, D.R., Sanberg, P.R., 2000. Adult bone marrow stromal cells differentiate into neural cells in vitro. Exp. Neurol. 164, 247–256.
Satoh, S., Toshima, Y., Ikegaki, I., Iwasaki, M., Asano, T., 2007. Wide therapeutic time window for fasudil neuroprotection against ischemia-induced delayed neuronal death in gerbils. Brain Res. 1128, 175–180.
Sauerzweig, S., Munsch, T., Lessmann, V., Reymann, K.G., Braun, H., 2009. A population of serum deprivation-induced bone marrow stem cells (SD-BMSC) expresses marker typical for embryonic and neural stem cells. Exp. Cell Res. 315, 50–66.
Shiokawa, M, Yamaguchi, T, Narita, M, Okutsu, D, Nagumo, Y, Miyoshi, K, Suzuki, M, Inoue, T, Suzuki, T., 2007. Effects of fasudil on neuropathic pain-like state in mice. Nihon Shinkei Seishin Yakurigaku Zasshi 27, 153–159 Japanese.
Someya, Y., Koda, M., Dezawa, M., Kadota, T., Hashimoto, M., Kamada, T., Nishio, Y., Kadota, R., Mannoji, C., Miyashita, T., Okawa, A., Yoshinaga, K., Yamazaki, M., 2008. Reduction of cystic cavity, promotion of axonal regeneration and sparing, and functional recovery with transplanted bone marrow stromal cell-derived Schwann cells after contusion injury to the adult rat spinal cord. J. Neurosurg. Spine 9, 600–610.
Song, S., Kamath, S., Mosquera, D., Zigova, T., Sanberg, P., Vesely, D.L., Sanchez-Ramos, J., 2004. Expression of brain natriuretic peptide by human bone marrow stromal cells. Exp. Neurol. 185, 191–197.
Sung, J.K., Miao, L., Calvert, J.W., Huang, L., Louis Harkey, H., Zhang, J.H., 2003. A possible role of RhoA/Rho-kinase in experimental spinal cord injury in rat. Brain Res. 959, 29–38.
Terada, N., Hamazaki, T., Oka, M., Hoki, M., Mastalerz, D.M., Nakano, Y., Meyer, E.M., Morel, L., Petersen, B.E., Scott, E.W., 2002. Bone marrow cells adopt the phenotype of other cells by spontaneous cell fusion. Nature 416, 542–545.
Wennersten, A., Meier, X., Holmin, S., Wahlberg, L., Mathiesen, T., 2004. Proliferation, migration, and differentiation of human neural stem/progenitor cells after transplantation into a rat model of traumatic brain injury. J. Neurosurg. 100, 88–96.
Woodbury, D., Schwarz, E.J., Prockop, D.J., Black, I.B., 2000. Adult rat and human bone marrow stromal cells differentiate into neurons. J. Neurosci. Res. 15, 364–370.
Woodbury, D., Reynolds, K., Black, I.B., 2002. Adult bone marrow stromal stem cells express germline, ectodermal, endodermal, and mesodermal genes prior to neurogenesis. J. Neurosci. Res. 69, 908–917.
Wright, K.T., El Masri, W., Osman, A., Roberts, S., Chamberlain, G., Ashton, B.A., Johnson, W.E., 2007. Bone marrow stromal cells stimulate neurite outgrowth over neural proteoglycans (CSPG), myelin associated glycoprotein and Nogo-A. Biochem. Biophys. Res. Commun. 354, 559–566.
Wu, S., Suzuki, Y., Ejiri, Y., Noda, T., Bai, H., Kitada, M., Kataoka, K., Ohta, M., Chou, H., Ide, C., 2003. Bone marrow stromal cells enhance differentiation of cocultured neurosphere cells and promote regeneration of injured spinal cord. J. Neurosci. Res. 72, 343–351.
Yano, S., Kuroda, S., Shichinohe, H., Seki, T., Ohnishi, T., Tamagami, H., Hida, K., Iwasaki, Y., 2006. Bone marrow stromal cell transplantation preserves gammaaminobutyric acid receptor function in the injured spinal cord. J. Neurotrauma 23, 1682–1692.
Ying, Q.L., Nichols, J., Evans, E.P., Smith, A.G., 2002. Changing potency by spontaneous fusion. Nature 416, 545–548.
Yoshihara, H., Shumsky, J.S., Neuhuber, B., Otsuka, T., Fischer, I., Murray, M., 2006. Combining motor training with transplantation of rat bone marrow stromal cells does not improve repair or recovery in rats with thoracic contusion injuries. Brain Res. 1119, 65–75.
Zhu, H., Mitsuhashi, N., Klein, A., Barsky, L.W., Weinberg, K., Barr, M.L., Demetriou, A., Wu, G.D., 2006. The role of the hyaluronan receptor CD44 in mesenchymal stem cell migration in the extracellular matrix. Stem Cells 24, 928–935.

JOURNAL OF NEUROTRAUMA 26:1–10 (July 2009)

DOI: 10.1089/neu.2008.0776

Wnt-Ryk Signaling Mediates Axon Growth Inhibition and Limits Functional Recovery after Spinal Cord Injury

Tomohiro Miyashita,[1,2] Masao Koda,[3] Keiko Kitajo,[1] Masashi Yamazaki,[2] Kazuhisa Takahashi,[2] Akira Kikuchi,[4] and Toshihide Yamashita[1,5]

Abstract

Wnt proteins are a large family of diffusible factors that play important roles in embryonic development, including axis patterning, cell fate specification, proliferation, and axon development. It was recently demonstrated that Ryk (receptor related to tyrosine kinase) is a conserved high-affinity Wnt receptor, and that Ryk-Wnt interactions guide corticospinal axons down the spinal cord during development. Here, we report that the Ryk-Wnt signal mediates the inhibition of corticospinal axon growth in the adult spinal cord. The expression of Wnt-5a is induced in reactive astrocytes around the injury site following a spinal cord injury. *In vitro*, Wnt-5a inhibits the neurite growth of postnatal cerebellar neurons by activating RhoA/Rho-kinase. In rats with thoracic spinal cord contusion, intrathecal administration of a neutralizing antibody to Ryk resulted in significant axonal growth of the corticospinal tract and enhanced functional recovery. Thus, reexpression of the embryonic repulsive cues in adult tissues contributes to the failure of axon regeneration in the central nervous system.

Key words: axon; regeneration; Rho; spinal cord injury; Wnt

Introduction

In the adult mammalian central nervous system (CNS), it is well established that injured axons exhibit very limited regenerative ability. Due to the lack of appropriate axonal regeneration, traumatic damage to the adult brain and spinal cord frequently causes permanent neuronal deficits. After a CNS injury, various neurite outgrowth inhibitors are present around the damaged site and are considered to be, at least in part, responsible for lesion-induced poor axonal regeneration and functional deficits. Among these inhibitors, myelin-associated glycoprotein, Nogo, and oligodendrocyte-myelin glycoprotein are well characterized (Yamashita et al., 2005). Downstream of these inhibitors, the activation of RhoA and its effector Rho-associated serine/threonine kinase (Rho-kinase), after the binding of these inhibitors to the corresponding receptors, has been demonstrated to be a key element for axonal growth inhibition (Mueller et al., 2005). In addition, recent publications propose roles for other proteins, including ephrin B3, Sema4D, and repulsive guidance molecule, in inhibiting axon regeneration following spinal cord injury (SCI) (Moreau-Fauvarque et al., 2003; Benson et al., 2005; Hata et al., 2006). These proteins are well known for their ability to repel axons during the developmental stages. During the development of the nervous system, outgrowing axons are often required to travel long distances in order to reach their target neurons. In this process, outgrowing neurites tipped with motile growth cones rely on repulsive and attractive guidance cues present in their local environment. Therefore, cues that repel axons during the developmental stage may act as inhibitory molecules for injured axons in adults.

Members of the Wnt family of proteins are key regulators of pivotal developmental processes that include patterning, the specification of cell fate, and the determination of tissue polarity (Ciani et al., 2005; Zou, 2004). In recent years, evidence has accumulated to suggest that Wnt proteins also play important roles in axon development during the formation of the nervous system (Zou, 2004). Wnt proteins have been demonstrated to be bifunctional axon guidance molecules and several Wnt proteins appear to mediate guidance of corticospinal tract (CST) axons along the spinal cord via repulsion (Liu et al., 2005). Wnt-1 and Wnt-5a are expressed in the mouse spinal cord gray matter, cupping the dorsal funiculus, in an anterior-to-posterior decreasing gradient along the cervical and thoracic cord. These Wnt proteins repel CST

Departments of [1]Neurobiology and [2]Orthopaedic Surgery, Graduate School of Medicine, Chiba University, Chiba, Japan.
[3]Togane Prefectural Hospital, Chiba, Japan.
[4]Department of Biochemistry, Graduate School of Biomedical Sciences, Hiroshima University, Hiroshima, Japan.
[5]Department of Molecular Neuroscience, Graduate School of Medicine, Osaka University, Osaka, Japan.

axons *in vitro* through a conserved receptor, Ryk, which is expressed in the CST axons. The posterior growth of CST axons is blocked by a neutralizing antibody to Ryk, thereby establishing that Wnt proteins are repulsive guidance cues for developing CST axons. These findings increase the prospects of navigation for severed axons in adults, and provide evidence to suggest that some repulsive guidance cues act as inhibitors of axon growth.

In the present study, we assessed whether Wnt proteins act as inhibitors of axon growth in the adult spinal cord. The expression of Wnt-5a increased following thoracic SCI in rats. Importantly, using a function-blocking antibody, we provide evidence that Wnt-Ryk inhibition promotes axon growth and functional recovery following SCI.

Methods

All the experimental procedures were approved by the Institutional Committee of Chiba University.

Surgical procedure

Anesthetized (2% halothane) female Sprague–Dawley rats (200–250 gm) underwent a laminectomy at the T9/T10 vertebral level, thereby exposing the spinal cord. We contused the spinal cords with an Infinite Horizon Spinal Cord Impactor (Precision Systems and Instrumentation, Fairfax, VA). The impact force was set at 200 kdyn. In order to perform the neutralizing antibody treatment in the animal model, the rats were fitted with an osmotic minipump (200 μl, 0.5 μl/h, administered for 2 weeks; Alzet 2002; Durect Corp., Cupertino, CA) immediately after SCI. These pumps were filled with control rabbit immunoglobulin G (IgG; 26 animals, 13.0 μg/kg/day, over a 2-week period; Sigma, Saint Louis, MO) or an anti-Ryk antibody (21 animals, 13.0 μg/kg/day, over a 2-week period; Abgent, San Diego, CA). The anti-Ryk antibody was raised against the extracellular domain of Ryk. The minipump was placed under the skin on the animal's back, and a silastic tube connected to the outlet of the minipump was placed under the dura at the spinal cord contusion site with its tip immediately caudal to the injury site. Fibrin sealants (Beriplast; ZLB Behring, King of Prussia, PA) were allowed to drip on the dura in order to anchor the tube that was protruding from the dura. Thereafter, the muscle and skin layers were sutured. The bladder was evacuated by manual abdominal pressure at least twice a day until the bladder function was restored. Sham-operated rats ($n = 6$) underwent laminectomy at the T9/10 vertebral level, thereby exposing their spinal cords. Minipumps that were filled with 0.85% saline and connected to silastic tubes were placed in three rats. Neither a minipump nor a silastic tube was placed in the other rats. Subsequently, the muscle and skin layers were sutured.

We used a section model to examine Wnt expression. The rats received a laminectomy at vertebral level T9/10, and the spinal cord was exposed. A no. 11 blade was used for the total section of the spinal cord, and the muscle and skin layers were sutured.

Tissue preparation and immunohistochemistry

For immunohistochemistry, tissues were obtained from an uninjured spinal cord and from spinal cords at 1, 3, and 7 days after the injury. After administering deep anesthesia using sodium pentobarbital, the animals were killed by perfusion with phosphate-buffered saline (PBS) followed by 4% paraformaldehyde. The animal's spinal cords were dissected, postfixed overnight in the same fixative, and cryopreserved in 20% sucrose in PBS. The spinal cord located 5 mm rostral and 5 mm caudal to the lesion site (10 mm long) was embedded in Tissue Tek OCT and immediately frozen in liquid nitrogen at −80°C. In addition, transverse sections were also collected from the spinal cord 10 mm rostral to the injury site. Using a cryostat, a series of 50-μm parasagittal or transverse sections were cut and mounted on poly-L-lysine (PLL)-coated Superfrost-Plus slides (Matsunami, Osaka, Japan). The sections were washed three times with PBS, then blocked with PBS containing 5% bovine serum albumin (BSA) and 0.1% Triton X-100 for 1 h at room temperature. The sections were incubated overnight with primary antibody at 4°C and washed three times with PBS. This was followed by incubation with fluorescein-conjugated secondary antibody (1:1000; Molecular Probes, Eugene, OR) for 1 h at room temperature. The anti-Wnt-5a antibody was prepared in rabbits by immunizing the animals with a synthetic peptide corresponding to the mouse Wnt-5a (Kurayoshi et al., 2006). A monoclonal anti-GFAP antibody (1:200; Chemicon, Temecula, CA), the monoclonal antibody (Tuj1) that recognizes the neuron-specific β-tubulin III protein (1:500; Covance, Berkeley, CA), or the anti-Ryk antibody was used as the primary antibody.

Neurite outgrowth assay

Cerebellar granule neurons (CGNs) from postnatal rats pups (P6–P10) were dissociated by trypsinization (0.25% trypsin in PBS for 10 min at 37°C), followed by resuspension

FIG. 1. Wnt-5a is induced in astrocytes and microglia/macrophages after spinal cord injury (SCI). (**A,B**) Wnt-5a is expressed in rat spinal cord neurons. Fixed tissues were obtained for immunohistochemistry from sham-operated (control) adult rat spinal cords. Parasagittal sections were stained with the anti-Wnt-5a antibody, and double stained with the anti-Tuj1 anti-Wnt-5a antibody. Wnt-5a is expressed in the axons in the white matter and neuronal cell bodies in the gray matter. Insets of the left panel correspond to high-magnification views in the right panels (upper insets correspond to upper panels). (**C,D**) The sections were also double stained with the anti-Wnt-5a anti–glial fibrillary acidic protein (GFAP) antibody (C) or the anti-Wnt-5a anti–myelin/oligodendrocyte-specific protein (MOSP) antibody (D). Wnt-5a was not expressed in astrocytes or oligodendrocytes. (**E**) Double labeling with anti-Tuj1 and anti-Wnt-5a antibodies shows colocalization 1 day after SCI. (**F,G**) Double labeling with anti-GFAP and anti-Wnt-5a antibodies shows colocalization in the epicenter area at 1 day (F) and 7 days (G) after SCI. (**H**) Immunohistochemistry for Ryk. Axial sections of injured spinal cord 10 mm rostral to the lesion site were obtained at 7 days after SCI, and were immunostained with the anti-Ryk antibody. The immunoreactivity for Ryk was found in the ventral part of the dorsal column. An inset of the left panel corresponds to a high-magnification view of the dorsal corticospinal tract (CST) in the right panel. Scale bar = 500 μm (left-side panels); 100 μm (right panel of H); 50 μm (others).

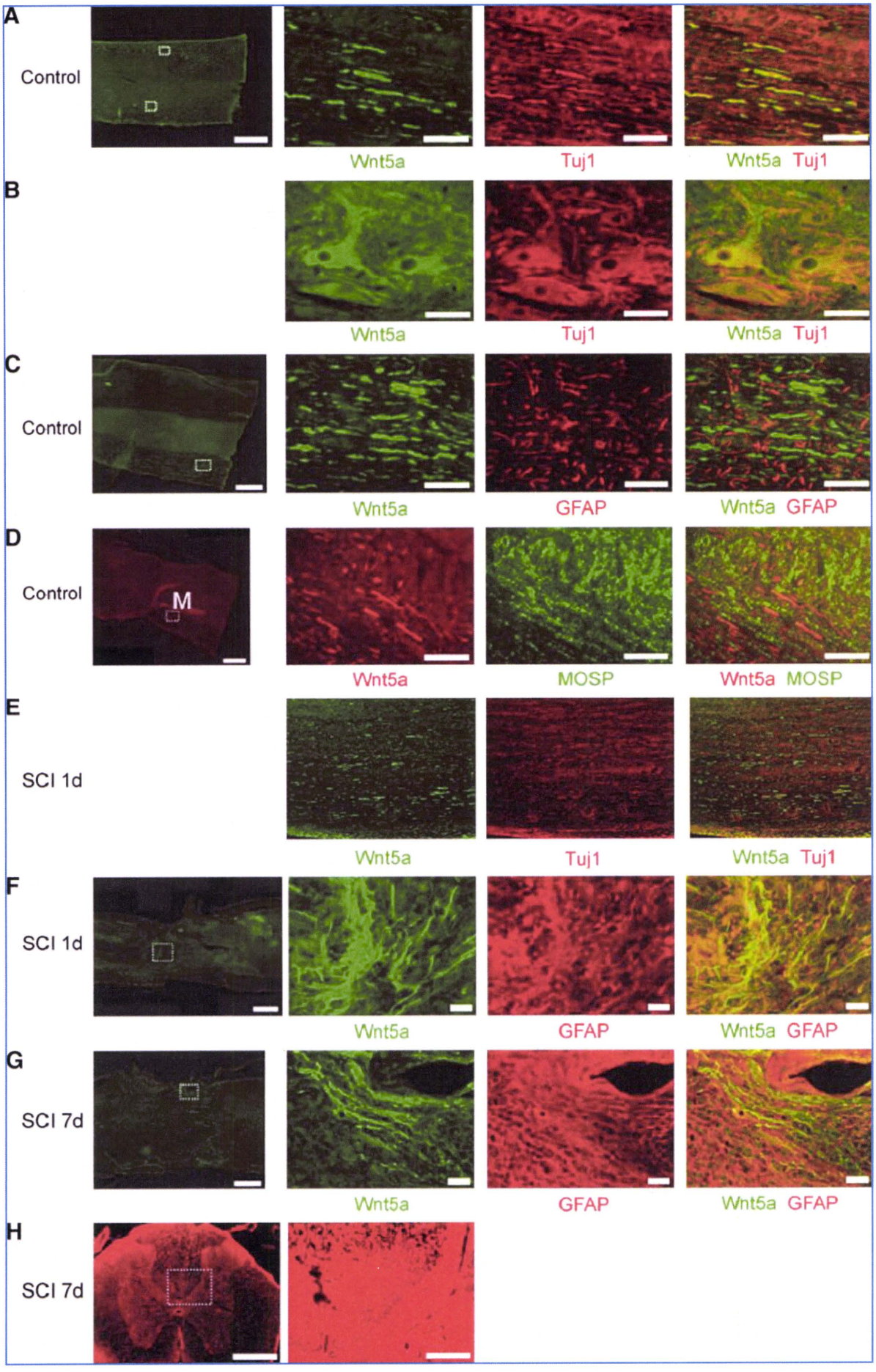
A
Control
Wnt5a
Tuj1
Wnt5a Tuj1
B
Wnt5a
Tuj1
Wnt5a Tuj1
C
Control
Wnt5a
GFAP
Wnt5a GFAP
D
Control
M
Wnt5a
MOSP
Wnt5a MOSP
E
SCI 1d
Wnt5a
Tuj1
Wnt5a Tuj1
F
SCI 1d
Wnt5a
GFAP
Wnt5a GFAP
G
SCI 7d
Wnt5a
GFAP
Wnt5a GFAP
H
SCI 7d

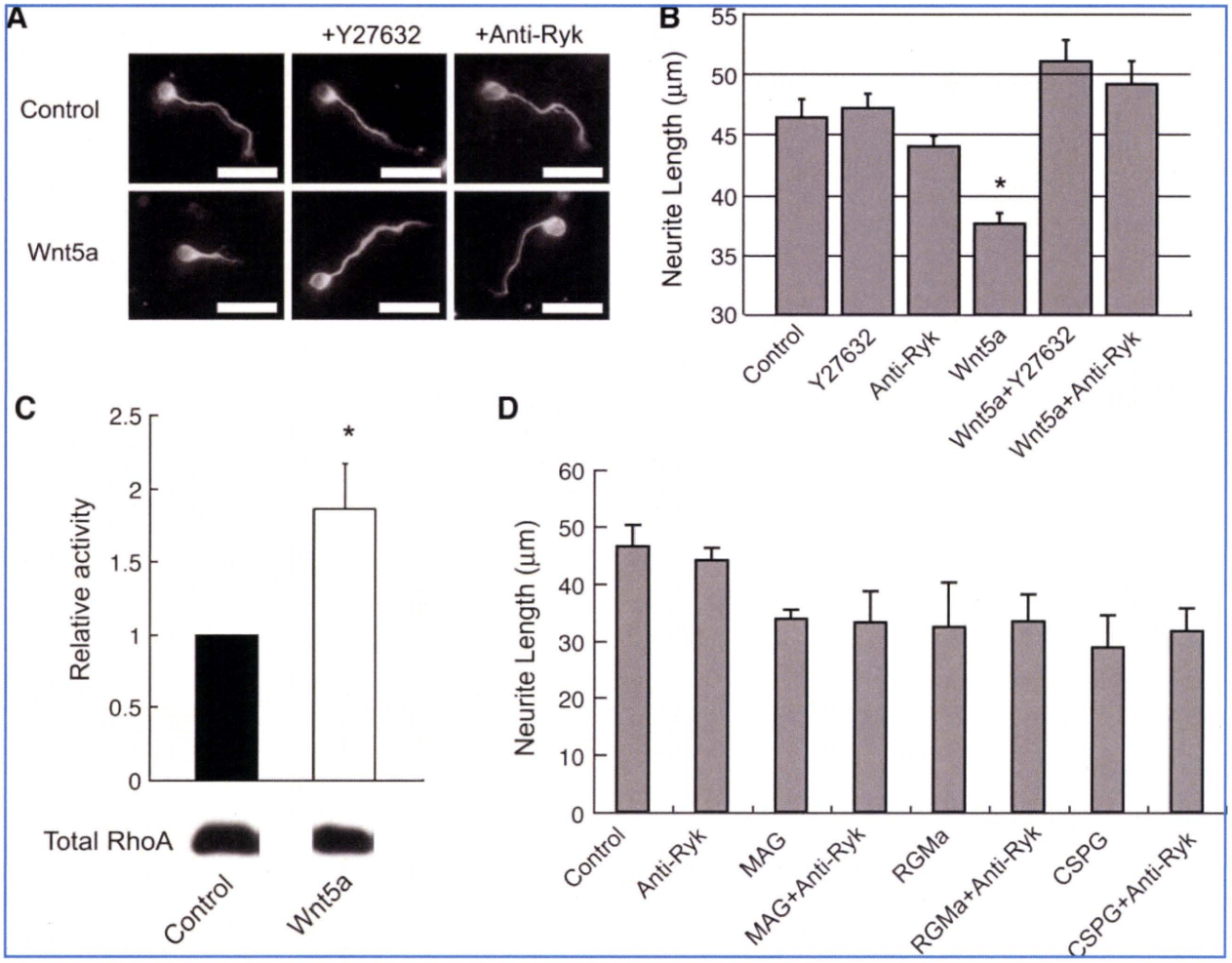

FIG. 2. Wnt proteins inhibit cerebellar granule neuron (CGN) neurite outgrowth. (**A**) CGNs were cultured on poly-L-lysine (PLL)–coated chamber slides for 24 h in a conditioned media with or without soluble Wnt-5a (90 ng/ml). Where indicated, Y27632 (10 μM) or the anti-Ryk antibody (0.5 μg/ml) was added. Scale bar = 25 μm. (**B**) The mean length of the longest neurite per neuron. The soluble form of Wnt-5a inhibits neurite outgrowth by a Rho-kinase-dependent mechanism and the anti-Ryk antibody reverses the effect of Wnt-5a. $^*P < 0.01$ (one-way analysis of variance [ANOVA] followed by Scheffe's multiple comparison test). Data are represented as the mean ± standard error of the mean (SEM) of three independent experiments. (**C**) Wnt-5a activates RhoA in the CGNs. CGNs were treated for 10 min with soluble Wnt-5a (90 ng/ml). The active fraction of RhoA was detected by a G-LISA Rho activation assay and the relative activity is shown. The bottom panel shows a western blot for total RhoA in the lysates. $^*P < 0.05$ (Student's *t*-test). Data are represented as the mean ± SEM of four independent experiments. (**D**) The anti-Ryk antibody does not abolish the effect of MAG, RGMa, or chondroitin sulfate proteoglycans (CSPG). The mean length of the longest neurite per neuron. CGNs were cultured on PLL-coated chamber slides for 24 h in a conditioned media with or without soluble MAG-Fc (20 μg/ml), RGMa (2 μg/ml), or CSPG (1 μg/ml).

in a serum-containing medium, trituration, and three washes with PBS. The cultures were grown in serum-free Dulbecco's modified Eagle's medium (DMEM). For the soluble Wnt-5a assays, neurons were plated on a conditioned media on PLL-coated chamber slides (Lab-Tek; Nalge Nunc International, Rochester, NY) and incubated for 24 h. Wnt-5a proteins were purified to near homogeneity by three successive column chromatographies (Kishida et al., 2004; Kurayoshi et al., 2006). The concentration of Wnt-5a were 90 ng/ml. Where indicated, 10 μM Y27632 (Mitsubishi Pharmaceuticals, Tokyo, Japan) was added to the cultures. For the neutralizing antibody assay, the anti-Ryk antibody (Abgent) was added to the culture at a concentration of 0.5 μg/ml. Where indicated, rat MAG-Fc chimera (25 μg/ml; R&D Systems), chicken extracellular chondroitin sulfate proteoglycans (CSPGs; the major components of this mixture are neurocans, phosphacan, versican, and aggrecan; Chemicon), or recombinant mouse RGMa (1 μg/ml; R&D Systems) were added. The cells were fixed in 4% (wt/vol) paraformaldehyde and immunostained with a monoclonal antibody (Tuj1) that recognized the neuron-specific β-tubulin III protein (1:1000; Covance). Subsequently, the length of the longest neurite for each β-tubulin III-positive neuron was determined. The neurite length of 100 neurons was measured for each experiment ($n = 3$).

RhoA activity assay

A G-LISA Rho activation assay kit (Cytoskeleton, Denver, CO) was used according to the manufacturer's recommendations. Where indicated, the cultures of the CGNs were incubated with Wnt-5a (90 ng/ml) for 10 min after which the cultures were grown in serum-free DMEM for 12–24 h. The protein concentrations of the cell lysates were equalized between 1.0 and 2.0 mg/ml. The surplus cell lysates were retained for further assay. The amount of the total Rho proteins was determined by western blotting using a monoclonal antibody against RhoA (Santa Cruz Biotechnology, Santa Cruz, CA).

Behavioral testing

Behavioral recovery was assessed in an open-field environment for 8 weeks after the injury by using the Basso-Beattie-Bresnahan (BBB) locomotor rating scale (Basso et al., 1995). Uninjured and sham-operated rats ($n = 6$) achieved full scores. The quantification was performed in a blinded manner by two observers.

Anterograde CST labeling

Six weeks after injury, descending CST fibers were labeled with biotin dextran amine (BDA), 10% in saline, 2.0 μl per cortex (molecular weight [MW] of 10,000; Molecular Probes) that was injected in the left motor cortex under anesthesia (coordinates: 0.5–2.5 mm posterior to the bregma, 2 mm lateral to the bregma, 1.5-mm depth). For each injection, 0.5 μl BDA was delivered for a 30-s period via a 15–20-μm internal diameter glass capillary attached to a microliter syringe (Hamilton, Reno, NV). In total, we examined and compared the regenerative responses of four control and seven anti-Ryk antibody-treated rats after SCI. The animals were killed by perfusion with PBS followed by 4% paraformaldehyde 14 d after the BDA injection. The animal's spinal cords were dissected, postfixed overnight in the same fixative, and cryopreserved in 20% sucrose in PBS. The spinal cord located between 5 mm rostral and 5 mm caudal to the lesion site (10-mm long) was embedded in Tissue Tek OCT. These blocks were sectioned (50 μm) in the sagittal or transverse plane, retaining each section. In both cases, the transverse sections were also collected from the spinal cord located more than 5 mm rostral and caudal to the injury site (15 control and 13 anti-Ryk antibody-treated rats). We used the transverse sections for quantification, and the sagittal sections for the presentation of the images. These sections were incubated for 1 h with Alexa Fluor 488-conjugated streptavidin (1:400; Molecular Probes) in PBS containing 0.05% Tween-20.

Data analysis

Fifty-micrometer-thick transverse sections (four control and seven anti-Ryk antibody-treated rats) were evaluated. For each section, the number of intersections of BDA-labeled fibers was counted from 4 mm above to 4 mm below the lesion site. The axon number was calculated as the percentage of the fibers observed 4 mm above the lesion, where the CST was intact. The distance beyond the epicenter of the lesion was scored as a positive distance, whereas the other regions were scored as negative distances.

Results

Expression of Wnt-5a in the adult rat spinal cord

We first investigated the distribution pattern of Wnt proteins in the adult rat spinal cord. We performed immunohistochemistry on fixed sections of uninjured spinal cords. In the uninjured spinal cord of adult rats, immunoreactivity to Wnt-5a was observed in the white matter and the signal was colocalized with the immunoreactivity to neuron-specific ß-tubulin III protein (Tuj1) (Fig. 1A), demonstrating that Wnt-5a was expressed in the spinal cord axons. The Wnt-5a

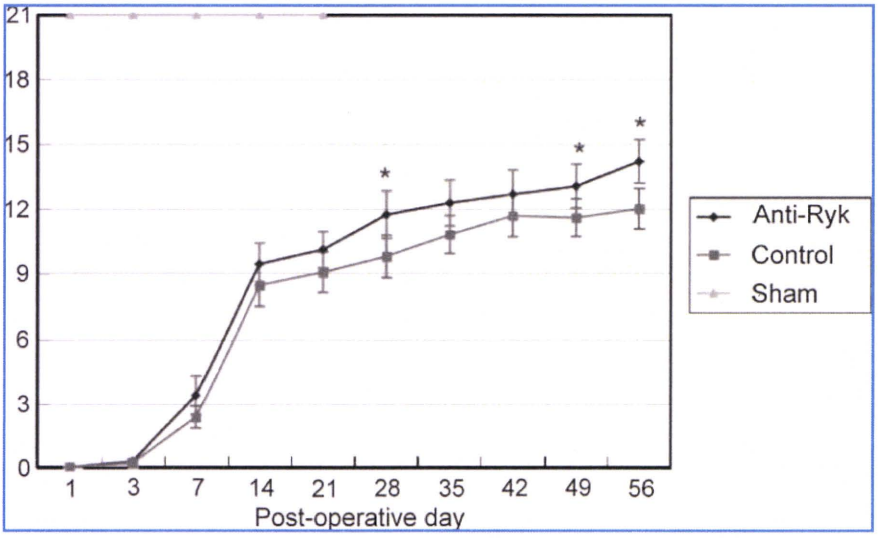

FIG. 3. The anti-Ryk antibody promotes locomotor recovery after spinal cord injury (SCI). The Basso-Beattie-Bresnahan (BBB) score was determined at the indicated times after thoracic contusion in the anti-Ryk antibody-treated (Anti-Ryk), control immunoglobulin G (IgG)–treated (Control), and sham-operated (Sham) rats. The mean ± standard error of the mean (SEM) of 21, 26, and six rats for each group, respectively. As indicated, the anti-Ryk antibody-treated group is statistically different from the control group. *$P < 0.05$ (Student's t-test) compared with the control.

immunoreactivity was also observed in the somata of Tuj1-positive neurons in the gray matter (Fig. 1B). Double immunostaining with the anti-Wnt-5a antibody and an antibody against the glial fibrillary acidic protein (GFAP) revealed no colocalization, demonstrating that Wnt-5a was not present in astrocytes (Fig. 1C). Double staining using anti-Wnt-5a anti–myelin/oligodendrocyte-specific protein (MOSP) antibodies demonstrated that Wnt-5a was not expressedin oligodendrocytes (Fig. 1D). Thus, Wnt-5a was expressed in neurons in the adult rat spinal cord.

Expression of Wnt-5a is up-regulated following SCI

In order to address whether Wnt proteins play a role in pathogenesis after CNS injury, we examined Wnt-5a expression following SCI in rats. We performed immunohistochemistry on fixed sections obtained at 1, 3, and 7 days after injury at the T9/10 vertebral level. Immunoreactivity to Wnt-5a was induced around the injury site during the observation period following surgery. We performed a double-label experiment after the injury to characterize the Wnt-5a-expressing cells. GFAP-positive and Wnt-5a-positive cells were detected in the epicenter area 1 day (Fig. 1F) and 7 days (Fig. 1G) after SCI, suggesting that Wnt-5a is expressed in the reactive astrocytes at the lesion epicenter. Immunoreactivity to Wnt-5a was observed in the white matter and the signal was colocalized with the immunoreactivity to Tuj1 (Fig. 1E). We did not observe MOSP-positive/Wnt-5a-positive cells in the lesion epicenter or in the adjacent white matter (data not shown), suggesting that oligodendrocytes do not express Wnt-5a.

We then obtained axial sections from injured spinal cord 10 mm rostral to the lesion site and assessed whether one of the receptors for Wnts (Ryk) was expressed in the spinal cord. The immunoreactivity for Ryk was found in the ventral part of the dorsal column—where the dorsal CST runs—at 7 days after SCI (Fig. 1H), although we found no significant immunoreactivity for Ryk in the dorsal column in the sham-operated rats (data not shown). These findings suggest that Ryk was expressed in the proximal axons of the CST after injury, which is consistent with the previous report (Liu et al., 2008).

Wnt-5a inhibits neurite outgrowth by a mechanism dependent on Ryk in vitro

A possible role of Wnt proteins in the pathogenesis of SCI is that they contribute to axonal inhibition. In order to address this hypothesis *in vitro*, we employed CGNs obtained from postnatal rats (P6–P10). These cells are frequently used for studying the function of the molecules that inhibit neurite growth (Yamashita et al., 2005). Although neurons from the adult cerebral cortex may be the optimal system for this type of study, to date we have been unsuccessful in culturing these neurons *in vitro*. For use in this assay, the Wnt-5a protein was purified to near homogeneity by three successive column chromatographies (Kishida et al., 2004; Kurayoshi et al., 2006). The CGNs from postnatal rats were cultured on PLL-coated slides in the presence or absence of Wnt-5a. At a concentration of 90 ng/ml, Wnt-5a significantly inhibited the neurite outgrowth of the CGNs (Fig. 2A,B). This inhibitory effect depended on Rho-kinase since the treatment of the CGNs with 10 μM Y27632—a specific inhibitor of Rho-associated protein kinase p160 ROCK (Uehata et al., 1997)—attenuated the effect of Wnt-5a, whereas Y27632 alone had no effect on neurite growth (Fig. 2A,B). To our knowledge, this is the first report to suggest that Wnt-5a inhibits neurite outgrowth, presumably by activating RhoA/Rho-kinase. Therefore, to directly assess whether RhoA is involved in the effect of Wnt-5a, the activity of RhoA was determined using the RhoA-binding domain of the effector protein, Rhotekin (Ren et al., 1999) and the G-LISA assay system (Fig. 2C). The assay revealed that, within 10 min of the addition of soluble Wnt-5a, extracts of the cells contained increased amounts of GTP-RhoA compared to those of the control cells. These results strongly suggest that Wnt-5a inhibits neurite outgrowth by a mechanism dependent on the activation of the RhoA/Rho-kinase pathway.

Ryk is a high-affinity receptor for Wnt-1, Wnt-3a, and Drosophila Wnt-5 (Yoshikawa et al., 2003; Lu et al., 2004). Ryk has been demonstrated to transmit repulsive signals in neurons (Liu et al., 2005; Schmitt et al., 2006; Keeble et al., 2006). This receptor is expressed in CGNs at a corresponding age (P6–P10) (Kamitori et al., 1999). These findings prompted us to examine whether Ryk is involved in the Wnt-mediated inhibition of CGN neurite growth. We used a polyclonal antibody for the ectodomain of Ryk (anti-Ryk) and tested whether the anti-Ryk antibody could block Wnt-5a-mediated inhibition. We observed that the addition of the anti-Ryk antibody (0.5 μg/ml) efficiently blocked the inhibitory effects of Wnt-5a at a concentration of 90 ng/ml (Fig. 2A,B), whereas the anti-Ryk antibody alone had no effect on neurite growth. However, the anti-Ryk antibody (0.5 μg/ml) did not influence the inhibitory effect of other neurite growth inhibitors, including MAG, RGMa, or CSPG (Fig. 2D), demonstrating the specificity of this neutralizing antibody. Therefore, Ryk is

FIG. 4. The anti-Ryk antibody promotes the regeneration/sprouting of corticospinal tract (CST) axons after spinal cord injury (SCI). (**A,C,E,G**) Representative transverse sections of the spinal cord located 10 mm rostral to the lesion site in the anti-Ryk antibody-treated (A,C) and control immunoglobulin G (IgG)–treated (E,G) rats. (C,G) Insets of (A) and (E), respectively, show high-magnification views of the dorsal CST. (**B,F**) Representative pictures of the spinal cord at 8 weeks after injury; the rostral site is indicated to the left. The anti-Ryk antibody-treated (B) or control IgG-treated (F) spinal cord at 8 weeks after the injury. (**D,H**) Higher magnifications of the boxed regions in (B) and (F), respectively. Anterograde-labeled CST fibers were observed caudally in rats treated with the anti-Ryk antibody (D), but not in the corresponding regions of the control IgG-treated rats (H). Scale bar = 500 μm (A,B,E,F); 200 μm (C,D,G,H). (**I**) The number of labeled corticospinal axons located 10 mm rostral to the lesion site in rats treated with the control IgG or the anti-Ryk antibody was measured by using the transverse sections. No significant difference was observed. (**J**) Quantification of the labeled CST fibers in seven anti-Ryk-treated and four control IgG-treated animals. Fifty-micrometer-thick transverse sections were evaluated. The *x*-axis indicates specific locations along the rostrocaudal axis of the spinal cord. The *y*-axis indicates the ratio of the number of biotin dextran amine (BDA)–labeled fibers at the indicated site to those at 4 mm rostral to the lesion site. $^*P < 0.01$ compared with the control (Student's *t*-test).